UNITED STATES DEPARTMENT OF THE INTERIOR
GEOLOGICAL SURVEY

Intracaldera Tuffs and Central-Vent Intrusion of the Mahogany Mountain Caldera, Eastern Oregon

Dean B. Vander Meulen [1]

Open-File Report 89-77

[1.] U.S. Geological Survey
Menlo Park, California 94025

1989

ACKNOWLEDGEMENTS

I would like to express my appreciation to several people at the U.S. Geological Survey for their willing assistance during the field-mapping phase of the study. Special thanks are extended to Mike Grubensky and Tom Vercoutere for their helpful field observations and comments. I am particularly grateful to Jim Rytuba who conceptualized the problem, formalized and focused my efforts, and provided insightful guidance throughout the study.

TABLE OF CONTENTS

LIST OF ILLUSTRATIONS

ABSTRACT

The Mahogany Mountain caldera is one of several volcanic centers in southeastern Oregon that erupted silicic peralkaline tuffs during the middle Miocene. The 15- by 20-km caldera structure coincides with a 25 mGal gravity low that is filled with an estimated 280 km^3 of ash-flow and air-fall tuff. An unusually well-preserved central-vent complex is exposed in the resurgent dome of the caldera. Facies changes within the caldera indicate the majority of the tuffs erupted from the central vent. Near-vent facies include, surge deposits, lag breccias, and ash-flow and air-fall tuffs containing abundant blocks.

Major- and trace-element data indicate that both the intracaldera tuffs and the vent intrusion erupted from a bimodal magmatic system consisting of high-silica comendite, and zoned intermediate comenditic trachyte. The high-silica melt that formed the upper part of the magma chamber appears to have evolved as an open system with a small compositional gradient. Unusually low Nb, Zr, and Y values are characteristic of rocks that erupted from this part of the magma chamber. In contrast, an extreme range of Nb, Zr, and Y values is characteristic of rocks erupted from the underlying intermediate-silica melt. This melt evolved in a closed magmatic system that developed a steep compositional gradient.

The central-vent eruption tapped both parts of the magma chamber simultaneously. Pyroclastic fragments that comprise the intracaldera tuffs and vent intrusion are a composite of both melts.

INTRODUCTION

Vents for major ash flow eruptions rarely have been identified in the geologic record (Smith, 1960). The lack of identifiable ash flow vent structures within most calderas suggests that large pyroclastic eruptions generally take place along the ring-fracture, through vents that are destroyed by caldera collapse (Lipman, 1984). However, this investigation indicates that a major caldera-forming eruption within the Mahogany Mountain caldera took place near the center of the caldera. The vent structure for this eruption was not destroyed during caldera collapse. A large part of the vent structure is presently exposed in the central resurgent dome of the caldera. The 0.6- by 1.6-km vent structure is filled with a rhyolite breccia intrusion and rhyolite dikes. At the margins of the vent complex the breccia locally grades into the intracaldera tuff. Geochemical correlations between the intracaldera tuff and vent intrusions, as well as facies changes in the tuff, indicate that the intracaldera tuffs erupted from the central vent.

From 1984 to the present, the U.S. Geological Survey has been conducting geologic field investigations in the Owyhee Uplands of eastern Oregon. These investigations are funded as part of a program to assess the mineral resources of possible wilderness lands in cooperation with the U.S. Bureau of Land Management, and as part of the Boise 2° quadrangle cooperative geologic mapping project with the Oregon Department of Geology and Mineral Industries. During these investigations, two caldera structures and a volcanic center were identified along the Owyhee Reservoir north of Mahogany Mountain. The topographic margins of these volcanic structures are illustrated in figure 1. Rocks associated with the calderas and volcanic center comprise the Owyhee volcanic field.

This investigation focuses on the intracaldera tuffs and intrusions of the Mahogany Mountain caldera. The caldera is located 12 km west of the Idaho state line adjacent to the Owyhee Reservoir (fig. 1). The 15- by 20-km elliptical caldera subsided during the eruption of the 15.5 million years before present (Ma), Leslie Gulch Ash-Flow Tuff Member of the Sucker Creek Formation (Kittleman and others, 1965; Kittleman, 1973). Major- and trace-

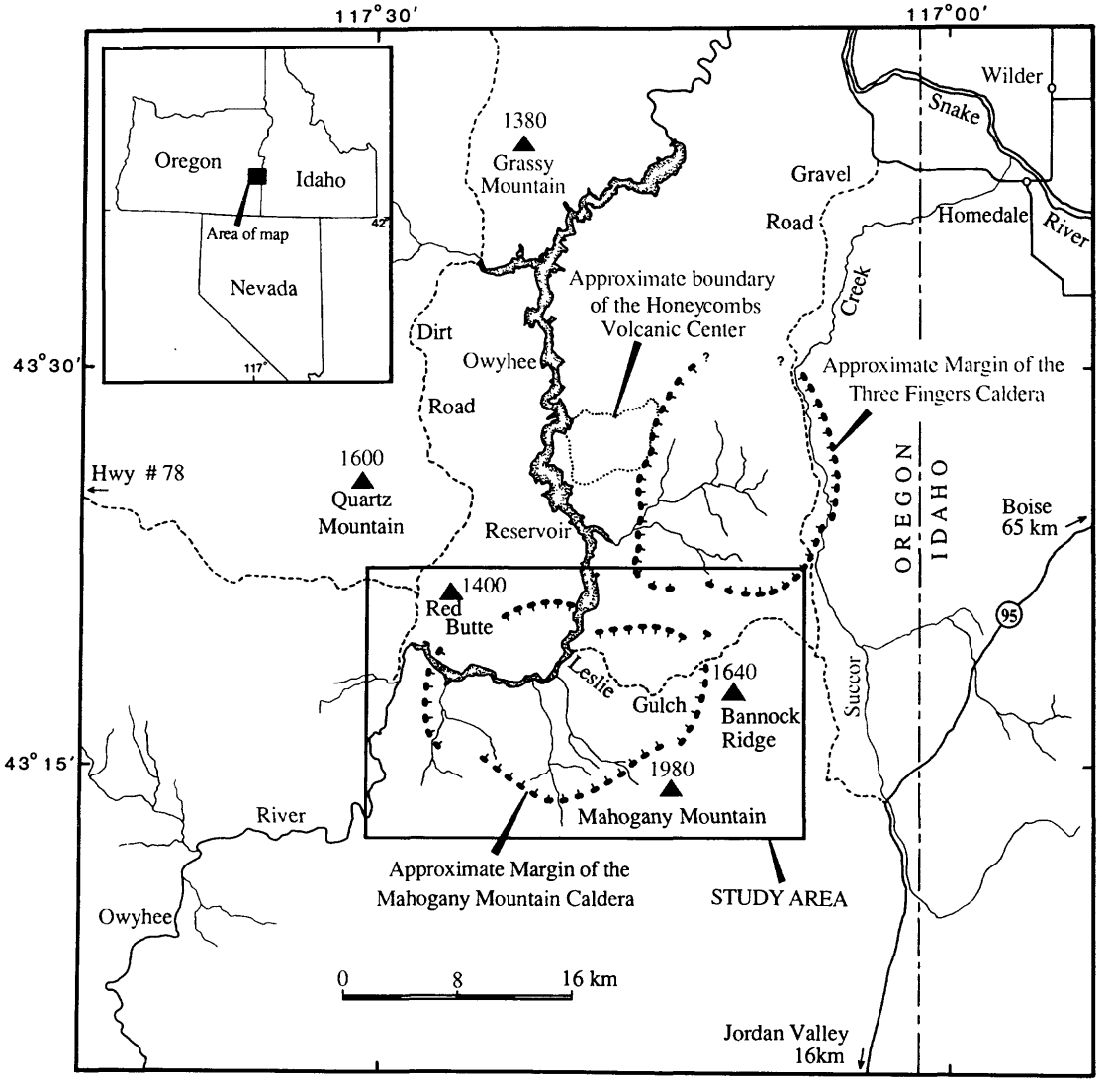

Figure 1. Index map of the study area showing the location of the Mahogany Mountain and Three Fingers calderas, and the Honeycombs volcanic center. Elevations in meters.

element geochemical data indicate that the tuff ranges from a high-silica comendite to an intermediate comenditic trachyte.

Post-collapse resurgent activity created a structural dome near the center of the caldera. A north-trending apical graben transects the central part of the resurgent dome. The caldera moat and central graben are filled by the tuffs of Spring Creek and Birch Creek. The tuff of Spring Creek is an 15.0-Ma ash-flow tuff that vented from the Three Fingers caldera, which is located 4 km northeast of Mahogany Mountain caldera (fig. 1). The tuff of Birch Creek is also an ash-flow tuff that vented from a caldera 15 to 25 km southwest of the study area. Two north-trending rhyolite dike systems crosscut the post-caldera tuffs and coincide with faults bounding the central graben. The youngest volcanic rocks associated with the caldera are porphyritic rhyolite dikes, plugs, domes, and flows that intrude the north and east margins of the caldera. Isolated outcrops of lacustrine sedimentary rocks unconformably overlie the tuffs in the eastern part of the caldera. The sedimentary rocks consist of fine-bedded tuffaceous sandstone, siltstone, and shale.

Location and Access

The study area, outlined in figure 1, encompasses 580 km^2 in the Owyhee Uplands of eastern Oregon. The area is located along the Owyhee Reservoir about 70 km west-southwest of Boise, Idaho and 32 km north of Jordan Valley, Oregon. The eastern part of the study area is accessible from U.S. 95 via an improved gravel road that parallels Succor Creek. The only access into the central part of the study area is from Leslie Gulch Road. This road enters the study area north of Bannock Ridge and continues west along Leslie Gulch to the Owyhee Reservoir. The western part of the study area is accessible from state highways 20 and 78 via two unimproved dirt roads that enter the region from the north and west (fig. 1). Several jeep trails and unimproved dirt roads enter the southern part of the study area along the south slope of Mahogany Mountain.

Topography and Climate

Maximum elevation in the study area is approximately 1980 m above sea level at Mahogany Mountain (fig. 1). Most of the mountain is drained by a radial pattern of intermittent creeks that flow north into Owyhee Reservoir and south into several small lakes. The northern part of the mountain is broken by an impressive arcuate scarp approximately 10 km in length. Topographic relief across the scarp from the mountain highlands to the caldera basin is approximately 500 m. Most of the caldera basin is drained by north- and northwest-flowing creeks (fig. 1) that empty into Leslie Gulch and the Owyhee Reservoir. The creeks have eroded deep gulches in the partly welded intracaldera tuffs.

The perennial Owyhee River which drains parts of southeastern Oregon, northern Nevada, and western Idaho has cut a major north-trending canyon in the southern part of the study area. Thirty kilometers north of the study area the canyon is dammed to form the Owyhee Reservoir.

Climate in the uplands is semiarid with 10 inches (25 cm) or less of annual precipitation. Sage brush and grasses are dominant at lower elevations. In the eastern part of the study area, groves of Juniper are common along creek bottoms and in protected gulches. Extensive groves of Mountain Mahogany and Aspen cover the highest elevations of Mahogany Mountain.

Previous and Present Investigations

During the 1960's and 70's, several large volume ash-flow tuff sheets were identified in eastern Oregon (Walker, 1970; Walker, 1977), but only a few of their eruptive sources were identified. During the last 10 years, several calderas (fig. 2) and their associated ash-flow tuff sheets have been identified in southeastern Oregon and northern Nevada (Rytuba and McKee, 1984).

Geologic investigations in the Owyhee region prior to 1984 included a reconnaissance geologic map by Kittleman and others (1967; scale 1:125,000), and a report outlining the general stratigraphy and descriptions of measured type sections

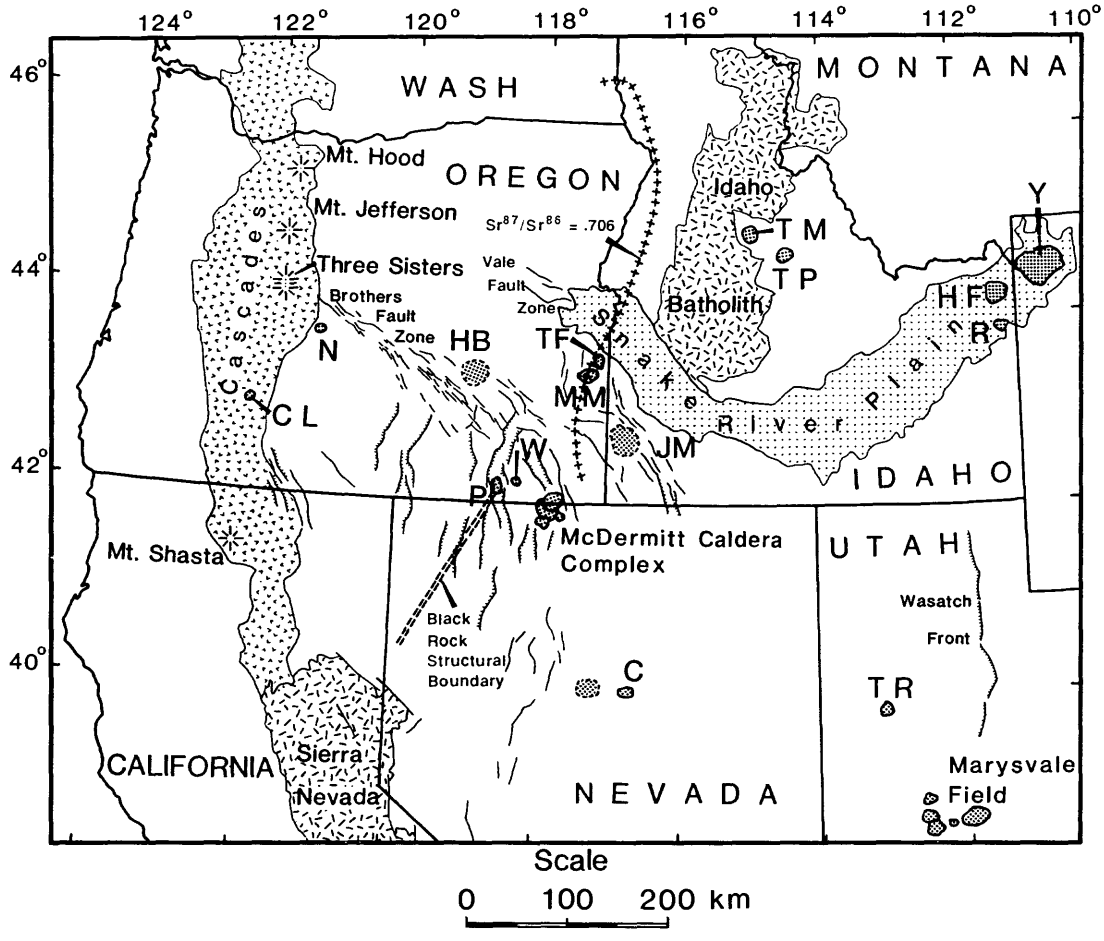

Figure 2. Location map of Cenozoic calderas (stipple pattern) showing their relation to selected geologic structures. Dashed circles shaded with stipple pattern indicate possible caldera structures. Heavy dashed line shows the Sr^{87}/Sr^{86} .706 boundary. Geology based on various maps (Lipman, 1984). C, Cortez 32 Ma; CL, Crater Lake 0.007 Ma; HB, Harney basin 6.4-9.2 Ma; HF, Henry Fork 1.2 Ma; JM, Juniper Mountain volcanic center 14 Ma; McDermitt caldera complex 15.6-16.1 Ma; MM, Mahogany Mountain 15.5 Ma; N, Newberry; P, Pueblo 15.8 Ma; R, Rexberg 7.3 Ma; TF, Three Fingers 15 Ma; TM, Timber Mountain 11 Ma; TP, Twin Peaks 45 Ma; TR, Thomas Range 39 Ma; W, Whitehorse 15 Ma; Y, Yellowstone 0.6 Ma.

(Kittleman and others, 1965). A preliminary evaluation of the mineral resources of parts of the study area were conducted by the Oregon Department of Geology and Mineral Industries (Gray and others, 1983).

Between 1984 and 1988, the U.S. Geological Survey conducted a combined geologic, geochemical, and geophysical survey of four wilderness areas located in the study area (Vander Meulen and others, 1987c; Vander Meulen and others, 1989). The Mahogany Mountain caldera (fig. 1) was recognized in 1984 by Rytuba and others (1985), and the Three Fingers caldera was recognized in 1987 by Rytuba and others (1989). Field investigations during 1985 involved detailed geologic mapping of a resurgent dome and vent complex located near the center of the caldera (Vander Meulen and others, 1987a,d) and reconnaissance mapping along the west side of the caldera (Vercoutere and others, 1987).

Geophysical investigations that include the study area are an aeromagnetic survey by Boler (1979) and an airborne radiometric and aeromagnetic survey by Geometrics, Inc. (1979). The latter was conducted during the U.S. Department of Energy's National Uranium Resource Evaluation (NURE) program. Gravity data for the region were interpreted by Lillie (1977) and Plouff (1987).

VOLCANIC SETTING

In the interval from 16 to 15 Ma, peralkaline rhyolite erupted from three known volcanic fields in the north-central Basin and Range physiographic province. These fields include; (1) the Mahogany Mountain and Three Fingers calderas in eastern Oregon (Rytuba, and others 1985; Rytuba and others, 1989), (2) the Pueblo and Whitehorse calderas, and McDermitt caldera complex in southeastern Oregon and northern Nevada (Rytuba and McKee, 1984;), and (3) the Silver City-Juniper Mountain volcanic center in southwestern Idaho (Ekren and others, 1984). Ash-flow tuff sheets associated with the calderas covered an estimated 25,000 km^2. Figure 2 shows the location of these calderas and their relation to major geologic structures. The calderas are aligned subparallel to an early Cenozoic continental-oceanic suture zone that extends from the Snake River Plain to north-central Nevada (fig. 2). Middle Miocene silicic volcanism was at least partially controlled by this preexisting deep-seated structural weakness. In Oregon, the suture zone is defined by the northeast-trending 0.706 Sr^{87}/Sr^{86} boundary (fig. 2). Silicic peralkaline volcanism and associated caldera genesis along this suture zone was probably related to regional NW-SE extension that developed in response to basin-and-range tectonism (Rytuba, 1989). In the north-central Basin and Range province, widespread development of horst and graben fault blocks began after the eruption of the 15-Ma tuff sheets (Rytuba and McKee, 1984). The Brothers and Vale fault zones (fig. 2) terminate extensional tectonism in this part of the province (Lawerence, 1976).

Regional Kinematics

The approximate northern boundary of the Basin and Range province is defined by the Brothers and Vale fault zones. The Brothers fault zone, located 80 km southwest of the study area (fig. 2), extends northwest 260 km across central Oregon from the Steens Mountain escarpment to the Cascade Range. At the surface, the 25-km-wide fault zone is delineated by a series of N. 55° W.-striking en echelon faults and fractures (Walker 1977; Lawerence, 1976). At Steens Mountain, tectonism associated with the Brothers

fault zone displaces 15.5- to 16.1-Ma Steens Basalt; here, the basalt flows are warped into a large northwest-striking faulted monocline (Walker, 1969). The Vale fault zone, located 70 km north of the study area (fig. 2), is an extension of the western Snake River Plain and is subparallel to the Brothers fault zone. The surface expression of the Vale zone is delineated by a series of N. 50° W.-striking normal faults (Walker, 1977). Satellite imagery (Lawerence, 1976) and geophysical data (Lillie and Couch, 1979) also show evidence of these major northwest-striking fault zones. The Brothers and Vale fault zones both show evidence of right-lateral displacement (Chaplet and others, 1986; Lawrence, 1976). Right-lateral displacement at the northern boundary of the Basin and Range province, indicates that less extension occurred north of the strike-slip fault zones, and greater extension and westward opening occurred south of the fault zones.

Timing of basin-and-range faulting between these strike-slip fault zones is partly controlled by the widespread distribution of 15-Ma ash-flow sheets of the Owyhee volcanic field. The age of these voluminous tuff sheets places a maximum age on the basin-and-range faulting that now dominates the topography of the study area. Initiation of block faulting in the area is further limited by a sequence of late Miocene sedimentary rocks and basalt flows that overlie the tuffs (Kittleman and others, 1967). In the western part of the study area, sedimentary rocks and basalt flows cap some of the ridges that bound the downfaulted valleys (Plate 1). Most of the major block faults in the study area trend between N. 10° W. and N. 10° E. The faults developed in response to regional east-west extensional tectonism that dominated the region during the late Miocene and Pliocene (Chaplet and others, 1986).

Topographic Margin of the Caldera

The Mahogany Mountain caldera is a 15- by 20-km structural basin that formed during the venting of an underlying magma chamber. Landslides that developed during caldera formation and subsequent erosion, modified the original caldera structural wall. The modified wall represents the topographic wall that encircles most of the caldera moat. The

caldera margin depicted in figure 1 and plate 1 parallels the base of the topographic wall. Several parts of the wall are offset by north-trending fault blocks. Normal displacement along the faults may have been complemented by 1.5 to 2 km of strike-slip movement.

The north topographic wall coincides with a 10-km-long west-trending scarp that extends east from the Owyhee Reservoir to Bannock Ridge (fig. 1). The wall is composed of precaldera sedimentary rocks and ash-flow tuff that erupted from the caldera (Plate 1). Two rhyolite domes and several rhyolite plugs and dikes intrude the northern margin and help delineate the topographic wall. Within the caldera, an estimated 200 m of post-caldera tuff is ponded against the length of the north wall. Cross section A-A' (Plate 1) illustrates some of the structural and stratigraphic relations along this part of the wall. Two parts of the north wall are offset by north-trending faults. The northwest part is displaced 2 km to the north along a structural break that follows the Owyhee Reservoir. This structural break is probably the southern extent of a large north-trending fault block. North of the study area, several large north-trending faults exposed on either side of the reservoir (Vander Meulen and others, 1987b) delineated other boundaries of the fault block. The northeast part of the topographic wall is broken by a 1- by 3-km north-trending embayment (Plate 1). The embayment probably formed when parts of the caldera floor subsided along preexisting north-trending faults. Tuffs associated with the caldera are ponded in the embayment, indicating that subsidence occurred before and (or) during caldera formation. In many calderas, similar embayments are related to slumping of wall rocks that were oversteepened during catastrophic collapse (Lipman, 1984).

The east topographic wall arcs south extending from the graben embayment to Mahogany Mountain. Sedimentary rocks exposed along this part of the wall are intruded by the rhyolite dome and flow complex of Bannock Ridge. Cross section B-B' (Plate 1) illustrates some of the structural and stratigraphic relations along this part of the wall. The rhyolite dome and flow complex that includes Bannock Ridge is the largest post-caldera ring-intrusion associated with the caldera.

Wall rocks exposed along the southern margin of the caldera are flows of highly resistant precaldera rhyolite. The wall is coincident with a 16-km scarp that arcs east-west along the north face of Mahogany Mountain. Relief along the southeast part of the wall locally exceeds 300 m. Here, parts of the present day wall closely parallel the original structural wall. Within the caldera, an estimated 400 m of post-caldera tuff ponded against the south wall.

The extreme west part of the topographic wall coincides with a 5-km-long arcuate fault scarp (Plate 1). The fault separates a massive basaltic intrusive complex from the caldera-forming outflow tuff; no intracaldera tuffs are exposed here. Extensional fault blocks are superimposed on the west wall of the caldera (Cross section B-B'; Plate 1). A large 9- by 20-km north-trending graben transects the west-central part of the caldera. A horst structure parallels the graben and forms a topographic high west of the caldera. Faults that delineate the west side of the graben and the east side of the horst coincide with the western structural wall of the caldera. North-trending normal faults exposed north of the Owyhee Reservoir (Plate 1) define the eastern part of the graben. Cross section B-B' (Plate 1) shows the width of the graben, and the estimated displacement along its bounding faults. Fault patterns in the northwest part of the study area (Plate 1) indicate that the graben opens to the north, becoming about 9 km across.

Resurgent Dome and Central Graben

The east-central part of the Mahogany Mountain caldera was structurally domed during post-collapse resurgence. Renewed rise of magma following caldera collapse commonly forms resurgent structures (Smith and Bailey, 1968). Uplift of the caldera floor domed and faulted intracaldera rocks and formed a topographic high in the eastern part of the caldera (fig. 3). A 0.8- by 5-km north-trending graben cuts the resurgent dome near the center of the caldera (Plate 1). The central graben probably formed in response to extensional stress across the crest of the resurgent dome. The intracaldera

Figure 3. View southeast across the Mahogany Mountain caldera. Photograph was taken from a ring-dome along the northwest margin of the caldera. The skyline in the right background is Mahogany Mountain. These highlands form the southern topographic wall of the caldera. The topographic expression of the resurgent dome includes the darker hills in the mid-background. The Spring Creek tuff forms the low hills on either side of the reservoir. The dark protruding rock mass on the far side of the reservoir is part of a north-trending rhyolite dike. The resurgent dome is approximately 5 km from the reservoir.

paleotopography is partly preserved due to infilling of the caldera moat by post-caldera tuffs. The tuffs filled the central graben and peripheral parts of the moat, ponding against the topographic high of the resurgent dome.

Timing of resurgent activity in the Mahogany Mountain caldera is bracketed by central-vent volcanism and the emplacement of north-trending rhyolite dike systems. The central vent erupted a great thickness of intracaldera ash-flow and air-fall tuffs that dipped away from their source. Cross sections constructed through the vent complex (fig. 4) indicate that the entire sequence of radial dipping tuff beds was tilted to the northwest. The radial pattern is restored when the sequence of tuff beds is tilted 15° to the southeast. Uplift of the caldera block that formed the northwestern part of the resurgent dome began after central-vent volcanism. Resurgent activity was probably nearly complete when post-caldera tuffs ponded around the central dome and filled the central graben.

Evolution of the Mahogany Mountain Caldera

The volcanic history of the Mahogany Mountain caldera parallels the classic stages of caldera development proposed by Smith and Bailey (1968). These stages include; (1) eruption of precaldera lavas, (2) caldera-forming voluminous ash-flow tuff eruptions, and (3) eruption of post-caldera ring-fracture and resurgent dome lavas and tuffs. Within the Mahogany Mountain caldera, these stages are characterized by; (1) an extensive precaldera dome and multiflow rhyolite complex that occupies Mahogany Mountain, (2) voluminous rhyolite ash-flow and air-fall tuffs that erupted concurrently with the collapse of the caldera, and (3) post-caldera rhyolite dikes, plugs, domes, and flows that were emplaced along the north and east margins of the caldera.

The precaldera rhyolite dome and flow complex was originally mapped as the Jump Creek Rhyolite by Kittleman (1973). Mapping during the present investigation has demonstrated that the rhyolite dome and flow complex is truncated by the caldera structure and therefore is older than the type locality of the Jump Creek Rhyolite. In this report, the precaldera silicic rocks are informally termed the rhyolite of

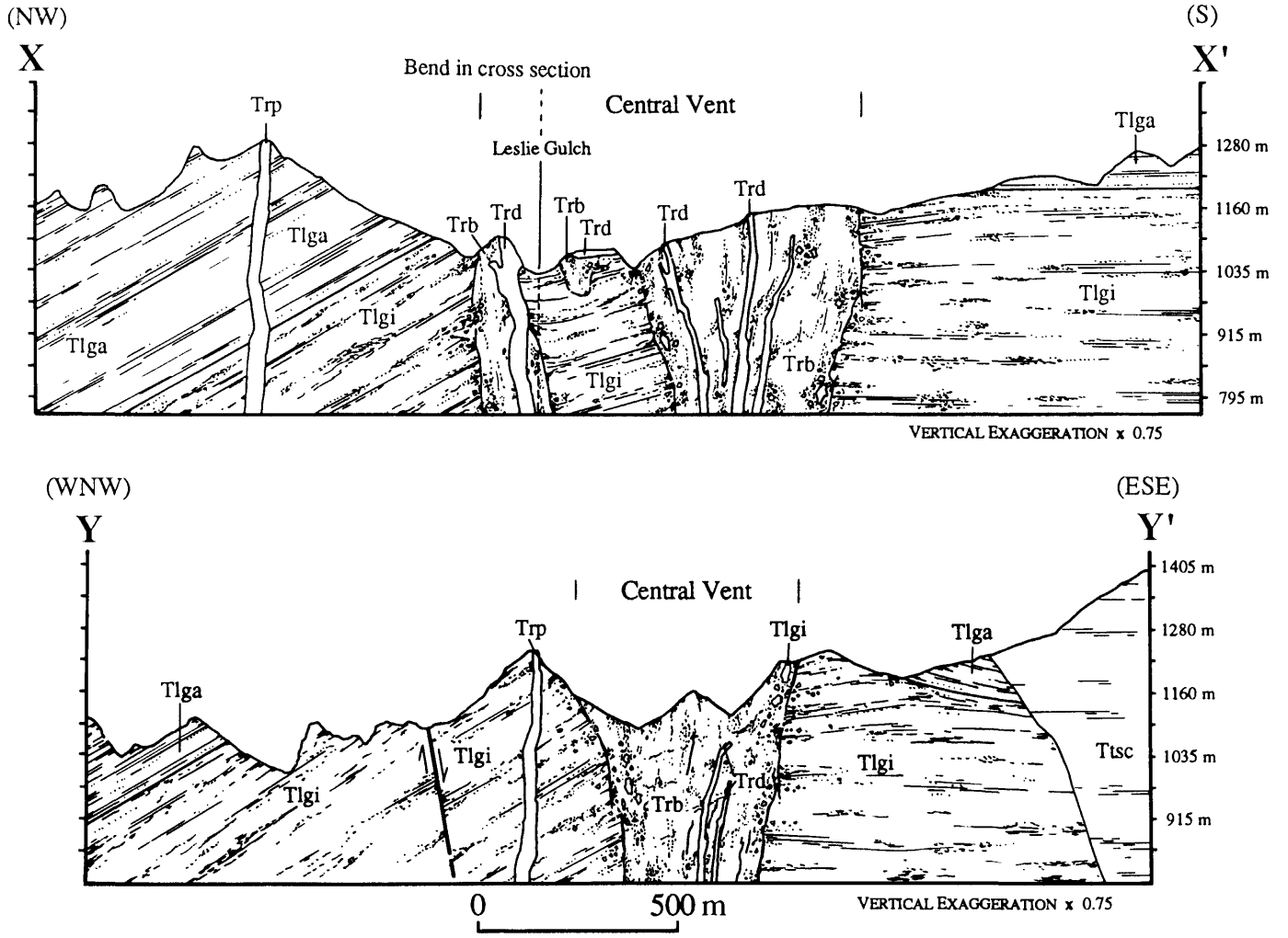

Figure 4. Geologic cross sections illustrating the central vent complex. See figure 5, page 16 for description of units and location of section lines.

Mahogany Mountain. The northern part of the dome and flow complex subsided with the formation of the Mahogany Mountain caldera. The southern part includes Mahogany Mountain and forms the southern topographic wall of the caldera.

The second episode of silicic volcanism is represented by large volumes of rhyolite ash-flow and air-fall tuff that erupted concurrently with the collapse of the caldera. The tuff has a potassium-argon age of 15.5 ± 0.5 Ma (Vander Meulen and others, 1987d). All age dates reported in this investigation were obtained from sanidine mineral separates. The total volume of tuff that erupted from the Mahogany Mountain caldera was approximately 360 km^3 (~215 km^3 dense rock equivalent; D.R.E.) and covered an estimated 2,800 km^2. Smith (1979) has shown that the depth to which calderas collapse can be derived by comparing the surface area of the caldera to the volume (D.R.E.) of the eruption. Using this method along with stratigraphic and structural field relations, the Mahogany Mountain caldera collapsed 1 to 1.3 km over an area of 210 km^2. The resulting depression was filled by an estimated 280 km^3 of caldera-forming tuff.

Silicic volcanism associated with caldera formation concluded with several rhyolite intrusions and flows. Two north-trending rhyolite dike systems intrude the floor of the caldera along both sides of a graben in the central resurgent dome. The dike systems cut all the intracaldera tuffs and are the youngest volcanic rocks in the caldera. A potassium-argon age from one of the dikes is 14.7 ± 0.4 Ma (Vander Meulen and others, 1987d). Several rhyolite domes and plugs that intrude the north and east margins of the caldera represent an episode of ring-fracture volcanism. A rhyolite dome and flow complex that intruded the east margin of the caldera has a potassium-argon age of 12.8 ± 0.3 Ma (Vander Meulen and others, 1987a). This ring-intrusion probably represents the last episode of volcanic activity associated with the caldera.

Central Vent Volcanism

Near the central part of the Mahogany Mountain caldera, a vent complex is exposed in the resurgent dome. Volcanic activity associated with the central vent is divided into four

general episodes. The first and second episodes are represented by a thick section of intracaldera ash-flow and air-fall tuffs. Intracaldera stratigraphy indicates that the explosive eruptions that deposited these tuffs progressed from a dominantly ash-flow eruption to a major plinian eruption. Eruption column density differences described by Sparks and Wilson (1976) can explain the sharp transition from ash-flow to plinian activity. Density differences in the column are controlled by the water and volatile content of the erupting magma. Lower gas contents in the column generate ash flows by gravitational column collapse (Sparks and Wilson, 1976). Eruptions with higher gas content are likely to generate air falls by greater convection motion in the column. Vent radius and temperature also have a significant influence on eruption style.

During the closing stages of the ash-flow and plinian eruptions, the vent conduit filled with a massive breccia intrusion. The third episode of volcanic activity associated with the vent is represented by the breccia intrusion. A geologic map (fig. 5) of the central-vent area illustrates the outcrop pattern of the breccia intrusion and the general shape of the vent. Along the margins of the vent, the intrusive breccia locally crosscuts and grades into the adjoining ash-flow tuff. These stratigraphic relations indicate that the intrusive episode was in part concurrent with the explosive eruptions.

The fourth and final episode of volcanism associated with the vent is represented by several rhyolite dikes and plugs that crosscut the vent breccia. Two cross sections constructed through the vent complex (fig. 4) illustrate the structural and stratigraphic relations between the intracaldera tuffs and vent intrusions. Major- and trace-element geochemical data presented later in this report indicate that the vent intrusions and intracaldera tuffs are comagmatic.

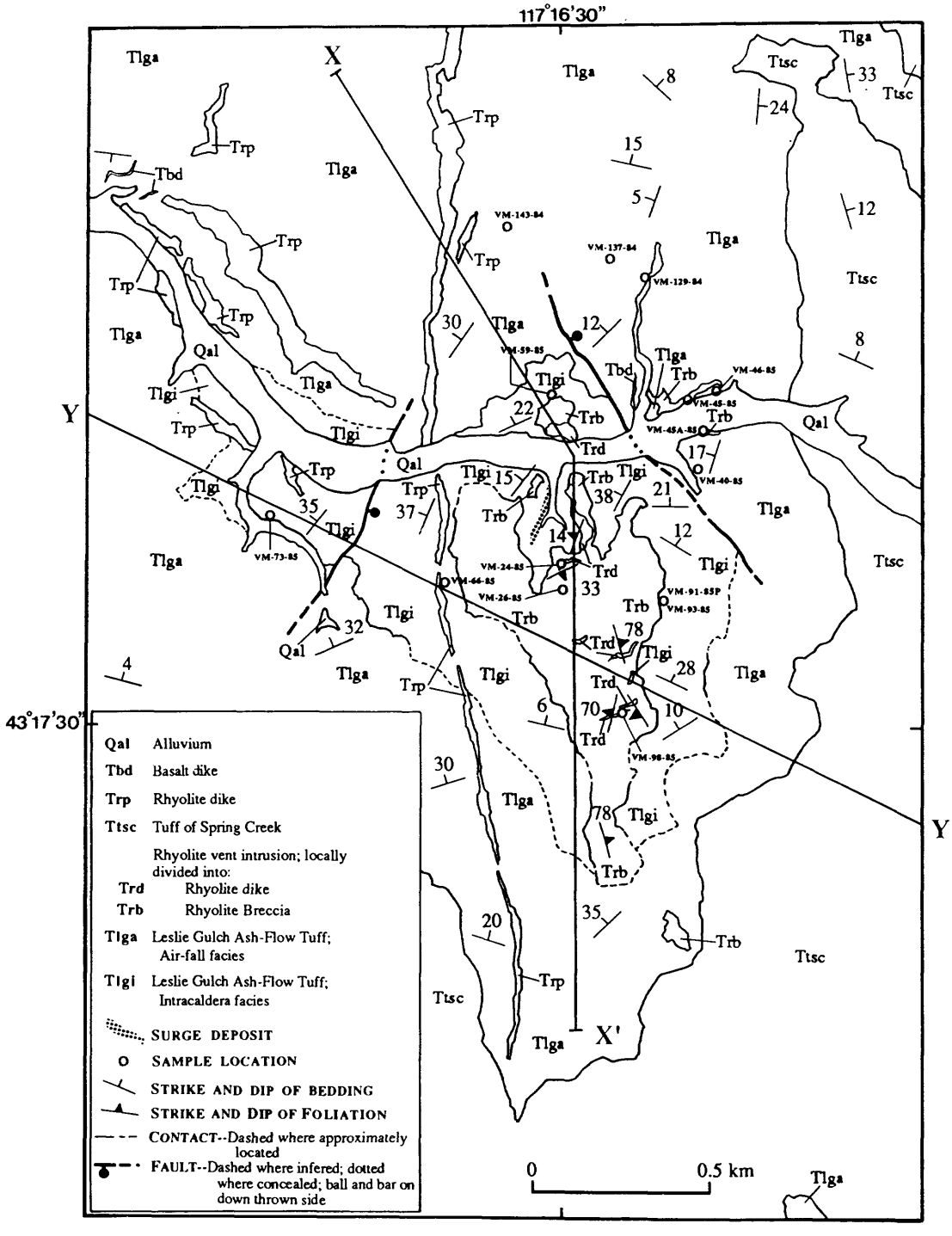

Figure 5. Geologic map of the central vent complex. Line segments X-X' and Y-Y' represent the surface trace of cross sections illustrated in figure 4. Area of the map is shown in plate 1.

GEOPHYSICAL INVESTIGATIONS

Geophysical investigations of the Mahogany Mountain caldera are based on interpretations of aeromagnetic and gravity data.

A contour magnetic map by Boler (1979) shows a linear magnetic low 5-to 7-km-wide trending approximately 35° east of north across the center of the study area. The low is probably associated with thick sections of weakly magnetic intracaldera tuff that fill the Mahogany Mountain caldera. Magnetic highs bound the magnetic low on the southeast and northwest sides. The southeastern magnetic high appears to be caused by a substantial thickness of precaldera rhyolites at Mahogany Mountain (Plate 1). The northwestern magnetic high has a substantial width (16 km) and form, and represents a causative rock mass at least 1500 m thick (Vander Meulen and others, 1989). The rock mass is concealed by relatively non-magnetic clastic rocks of the Sucker Creek Formation and the Deer Butte Formation (Kittleman and others, 1967).

Gravity data for the region are available from the National Geophysics Data Center (1984). The bulk of the data were obtained from an earlier survey conducted by students at Oregon State University. The earlier survey was described and generally interpreted in a thesis by Lillie (1977). Ten additional gravity stations were located within and near the study by Plouff (1987). Average spacing for these stations is 1.5 to 5 km. The complete set of data is presented as a contoured Bouguer anomaly map (fig. 6) with a contour interval of 2 milligals (mGal) and a reduction density of 2.67 g/cm^3.

In the study area, three coalescing gravity lows are associated specifically with the Mahogany Mountain caldera. The coalescing lows of about 10 mGal essentially coincide with the caldera (fig. 6). The southern edge of the gravity anomaly generally follows the topographic wall of the caldera along Mahogany Mountain but locally extends beyond the caldera margin. The northern extension of the gravity low (fig. 6) probably reflects a subsided wedge of tuffaceous sedimentary rock, and a substantial thickness of ash-flow and air-fall tuff that fill the Three Fingers caldera and Honeycombs volcanic center

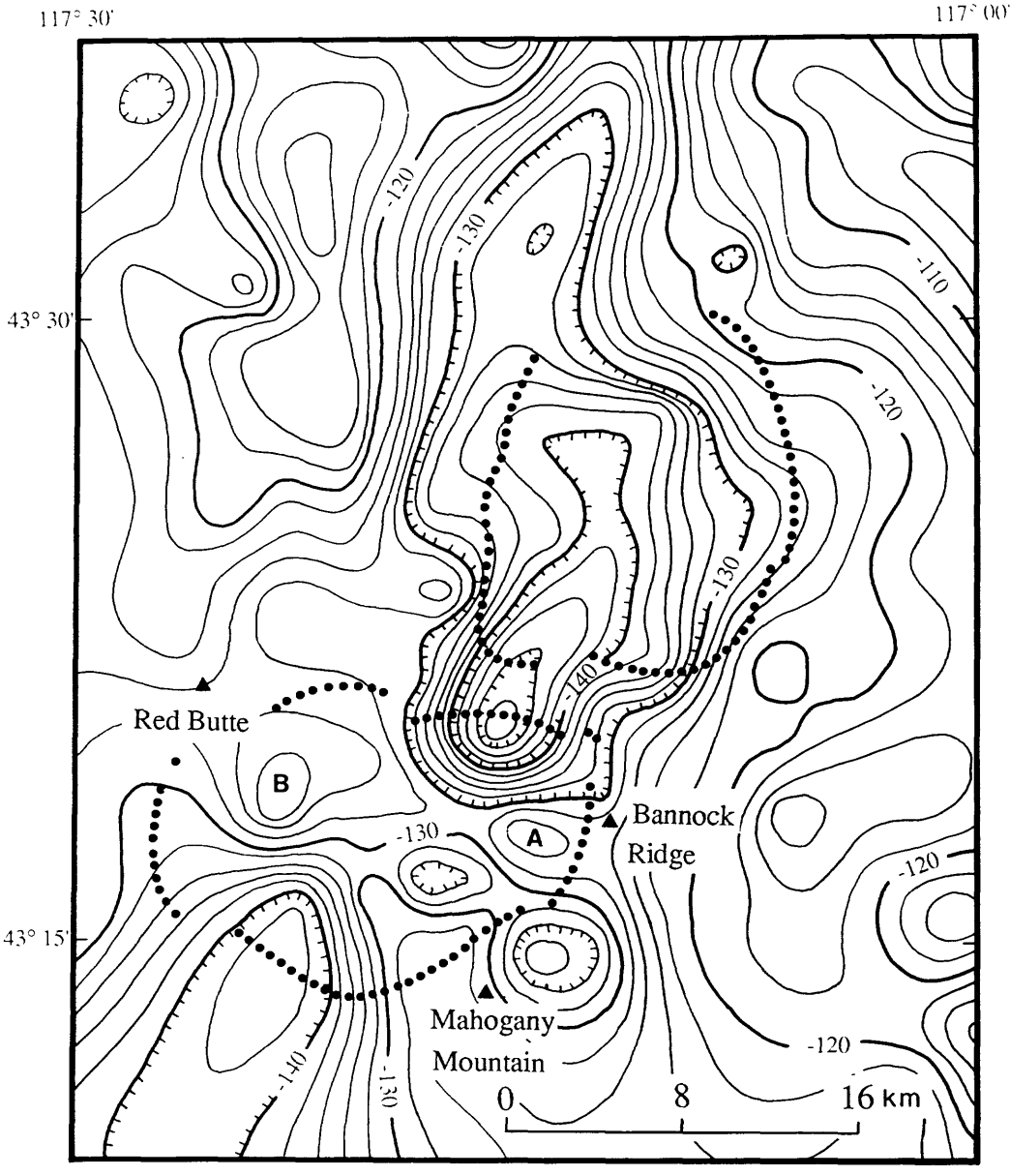

Figure 6. Bouguer gravity anomaly map of the Owyhee volcanic field, eastern Oregon. Heavy dotted lines depict the approximate margin of the Mahogany Mountain caldera (south) and the Three Fingers caldera (north). Closed gravity contours labeled "A" and "B" are discussed in the text. Gravity contour interval is 2 milligals.

(Vander Meulen and others, 1987b). The north-trending gravity low that includes both calderas and the volcanic center, reflects a caldera complex approximately 35 km long by 15 km wide.

A small closed gravity contour (-126 mGal) that corresponds to a gravity high in the eastern part of the Mahogany Mountain caldera (A; fig. 6) is probably caused by the central-vent intrusion and resurgent dome. The intrusion and resurgent dome caused local thinning of low-density intracaldera tuffs (Plate 1). A second closed gravity contour (-124 mGal) is associated with a gravity high in the west-central part of the caldera (B; fig. 6). In this area, several intermediate plugs, dikes, and sills have uplifted and intruded intracaldera tuffs.

A linear gravity high trending north-south along the northwest side of the caldera complex is part of a longer feature extending on strike at least 40 km farther north. North of the study area, Lillie and Couch (1979) interpreted similar north-south-trending anomaly gradients as normal faults separating horst and graben blocks. The linear feature along the northwest side of the caldera complex is probably the gravity expression of one of these major north-trending fault zones (Vander Meulen and others, 1989).

INTRACALDERA STRATIGRAPHY

During this investigation, 8 major rock units were mapped within the Mahogany Mountain caldera. The stratigraphically lowest exposed rocks in the caldera are located in the eastern uplifted part of the caldera. The rocks form a 350-m-thick interbedded sequence of ash-flow and air-fall tuffs, and surge deposits. A comagmatic rhyolite vent complex located in the central part of the caldera intrudes and grades into the tuffs. The vent complex consists of intrusive breccias crosscut by rhyolite dikes. Following collapse and resurgence of the Mahogany Mountain caldera two post-caldera rhyolite ash-flow tuffs erupted from nearby calderas and ponded in the caldera moat. The post-caldera tuffs are exposed in the eastern and southern parts of the caldera. The stratigraphic relation between the caldera-forming tuffs and post-caldera tuffs is illustrated in figure 7. Rhyolite and basalt dikes and plugs intruded the entire sequence of intracaldera volcanic rocks. Lacustrine sedimentary deposits are the youngest rocks exposed in the eastern part of the caldera. The western part of the caldera is buried by a thick sequence of fluviatile and lacustrine sedimentary rocks, basalt flows, and landslide deposits.

The intracaldera ash-flow and air-fall tuffs were originally mapped as a single ash-flow tuff unit, named the Leslie Gulch Ash-Flow Tuff Member of the Sucker Creek Formation (Kittleman and others 1965; Kittleman, 1973). On the basis of recent mapping (Vander Meulen and others, 1987d) the Leslie Gulch Ash-Flow Tuff has been redefined and subdivided into three facies; they include: (1) outflow facies consisting of ash-flow tuff exposed outside the caldera; (2) intracaldera facies consisting of ash-flow and air-fall tuff geographically restricted to the caldera; and (3) air fall facies consisting of air-fall tuff exposed within and adjacent to the caldera. All three facies were deposited during the collapse of the Mahogany Mountain caldera.

The post-caldera ash-flow tuffs were also originally included as part of the Leslie Gulch Ash-Flow Tuff. During this investigation the post-caldera tuffs were separated and mapped as two different units. The older of the two tuffs was named tuff of Spring Creek by Rytuba and others (1985). The younger of the two tuffs was named tuff of Birch Creek by Plumley (1986).

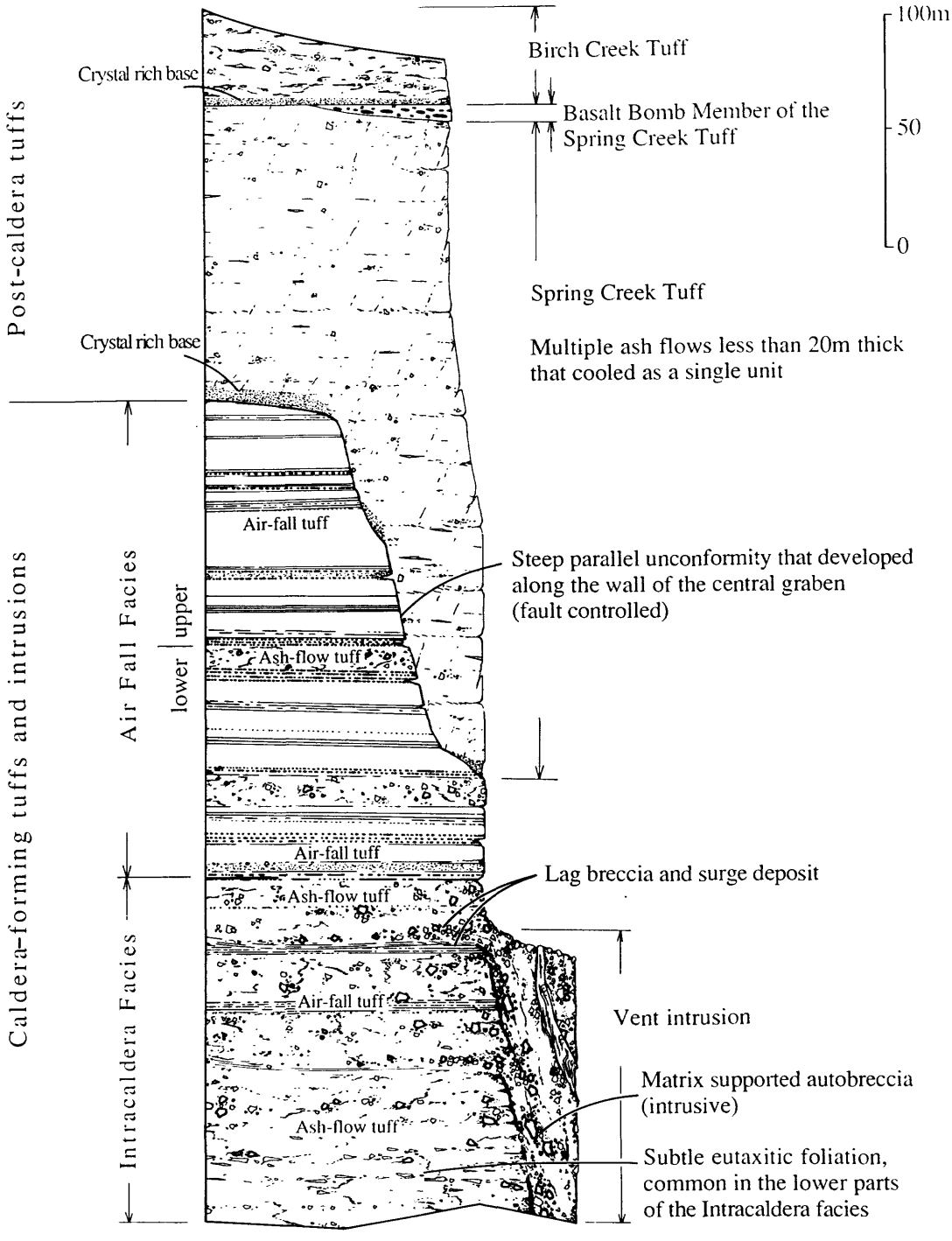

Figure 7. Schematic stratigraphic section illustrating the tuffs that fill the Mahogany Mountain caldera. The relation between intracaldera facies and the vent intrusion is depicted in the lower part of the section.

Rhyolite and basalt intrusions, and sedimentary rocks exposed in the eastern part of the caldera were also originally mapped as part of the Leslie Gulch Ash-Flow Tuff by Kittleman and others (1967). During this investigation these rocks were divided from the Leslie Gulch Ash-Flow Tuff and redefined accordingly.

Leslie Gulch Ash-Flow Tuff

Outflow Facies

Outflow facies consist of ash-flow tuff and several smaller air-fall tuffs, all of which erupted from the Mahogany Mountain caldera. The tuffs are exposed north and west of the caldera (Plate 1) and cover approximately 70 km^2. The ash-flow tuff cooled as a single unit that has a minimum thickness of 85 m along the north rim of the caldera. The tuff locally exceeds 350 m were it ponded in a paleovalley 6 km north of the caldera. Most of the outflow facies west of the caldera are buried by younger sedimentary rocks, although Plumley (1986) reported a 300-m-thick section exposed in the Owyhee River Canyon, 8 km southwest of the caldera.

The basal part of the outflow facies is made up of green to white, fine-grained, welded, vitric air-fall tuff that grades up into discontinuous black vitrophyre. Above the vitrophyre, the outflow facies consists of grayish-yellow to greenish-brown, welded, ash-flow tuff. The lower part of the ash-flow tuff contains blocks and lithic fragments of siltstone and sandstone. The size and abundance of blocks and lithic fragments varies greatly throughout the unit depending on proximity to the caldera vent. The distribution of pumice fragments shows a similar pattern where size and concentration increase toward the source. Flattened pumice fragments and distorted vitric structures are associated with secondary flow foliation in the lower more densely welded part of the ash-flow tuff. Secondary flow features are common near the base of the unit where heat and compression were greatest.

Internal stratigraphy of the outflow facies is relatively consistent. The unit is generally massive and unsorted containing only crude layering, although parts of the tuff grade up into well-

bedded air-fall tuff. The upper air-fall tuff is partly welded to nonwelded and typically contains pumice and lithic fragments similar to the underlying ash-flow.

Crystal content ranges from 20 percent near the base of the ash-flow tuff to less than 5 percent in the upper air-fall tuff. Phenocrysts are less than 3 mm across and include 2 to 15 percent sanidine, 2 to 5 percent quartz, and minor alibite. Sanidine and quartz grains commonly contain embayment structures filled with a devitrified groundmass. Glass shards as well as the groundmass are typically devitrified to fine-grained aggregates of cristobalite and feldspar. Pore spaces in the pumice fragments and other large vitric structures contain vapor-phase intergrowths of feldspar and quartz.

Intracaldera Facies

Intracaldera facies is made up of ash-flow tuff and several interbedded air-fall tuff and surge deposits that have a minimum thickness of 150 m and cover a total of 1.5 km^2. The tuffs were deposited during collapse of the Mahogany Mountain caldera, and are geographically restricted to the caldera. Tuffs of the intracaldera facies crop out in the deeply eroded resurgent core and along the west side of the Owyhee Reservoir (Plate 1). An estimated 600 to 900 m of intracaldera facies filled the Mahogany Mountain caldera during caldera collapse. Cross sections constructed through the caldera (Plate 1) illustrate the structural and stratigraphic relations of this facies.

The intracaldera facies is made up of several successive ash flows that cooled as a single unit; the base of this composite unit is not exposed. Plate 2 illustrates the upper 80 m of intracaldera facies that crops out approximately 150 m northwest of the vent complex. In this area, the lowest exposed part of the intracaldera facies is made up of pale-yellow to grayish-yellow ash-flow tuff. The tuff contains unsorted ash, pumice and lithic lapilli, and pumice blocks. Partly flattened pumice lapilli and blocks form a crude eutaxitic foliation.

Surge Deposit. In the northern part of the vent complex, a surge deposit stratigraphically overlies and cuts the ash-flow tuff. The location of the surge deposit is depicted as a stippled pattern

in figure 5. The deposit is confined to a 6-m-deep by 12-m-wide U-shaped channel. From bottom to top the main channel contains; (1) planar-parallel and massive beds, (2) sandwave beds, and (3) planar-parallel beds. The lower planar-parallel and massive beds consist of sorted ash and partly sorted ash and lapilli. Figure 8 shows exposures of the planar-parallel beds. Crystal settling within the surge cloud produced concentrated layers of crystals in the upper part of this unit. Planar-parallel and massive beds are commonly deposited at distal or intermediate distances from their source, at low energy levels (Wohletz and Sheridan, 1979). Sandwave beds are exposed near the stratigraphic center of the surge channel and contain a variety of features such as dunes, cross-beds, and backset and foreset cross-laminations. Dune amplitudes range from 25 to 75 cm, and cross-bed sets range from 10 to 100 cm thick. The sandwave beds are made up of unsorted ash, pumice and lithic lapilli, and rounded lithic blocks (fig. 9). Sandwave beds are thought to form close to the source by turbulent flow under high energy conditions (Wohletz and Sheridan, 1979). A lithic breccia unit composed of cognate tuff blocks 20 to 60 cm in diameter, is entrained near the top of the surge channel (fig. 9). The breccia unit has a maximum thickness of 3 m and contains subangular blocks at its closest point to the vent complex. The breccia unit is interpreted as a near-vent lag breccia similar to those described by Druitt and Sparks (1982). Approximately 50 m north of the vent, the breccia consists of well-rounded tuff blocks that disperse into sandwave beds (fig. 8). Planar-parallel beds consisting of sorted ash and pumice lapilli are exposed at the top of the channel between the lag breccia and an overlying ash-flow tuff.

Parts of the surge deposit can be traced laterally across discontinuous outcrops to exposures 150 m northwest and 400 m west of the vent complex. These deposits are planar-parallel beds 1 to 3 m thick consisting of ash and sorted lapilli. Wohletz and Sheridan (1979) indicate that planar beds result from normal gravity fallout in the distal part of a flow. Planar beds are commonly deposited at the terminus of avalanching flows where flow energy has dropped to a minimum (Fisher and Schmincke, 1984).

Figure 8. Near-vent surge deposit showing flow direction. Lower planar-parallel beds have been cut and scoured by the overlying high energy sand-wave beds and lithic breccia. Detritus settled out of the high energy flow and collected on the lee side of the rounded block. Flow direction was from left to right. Hammer is 40 cm long.

Figure 9. Near-vent surge deposit showing broad amplitude sand-wave beds and lithic breccia deposit. The light tan sand-wave beds in lower part of the photograph have been scoured by the overlying breccia deposit. Hammer is 40 cm long.

Ash-Flow Tuff. Stratigraphically above the surge deposit is a grayish-yellow to brownish-yellow ash-flow tuff. Tephra size, composition, and abundance varies widely throughout the partly welded ash-flow tuff. Generally, near the base of the tuff a subtle eutaxitic foliation is defined by less abundant, flattened, pale-yellow pumice fragments. The middle and upper parts of the tuff are nonwelded to partly welded and contain abundant angular, unflattened, orangish-brown pumice fragments and light green, juvenile, lithic fragments. Pumice and lithic fragments are commonly 2 to 4 cm across, becoming larger and more abundant near the vent complex. Orangish-brown pumice fragments are partly altered to clays and form pitted features in the tuff (fig. 10). Pale yellow pumice fragments are less altered and form positive relief on the tuff. Near the vent complex, blocks of medium-grey banded rhyolite 0.5 to 1 m across (fig. 11) are randomly distributed throughout the ash-flow tuff. Color and texture of the banded blocks is similar to the rhyolites that form the vent complex. The largest blocks are made up of brecciated rhyolite, identical to the vent breccia (following section).

The individual ash-flow units that make up most of the intracaldera facies are generally poorly sorted and nonbedded, containing crude discontinuous layers of pumice and lithic fragments. A near-vent ash-flow tuff shown in figure 12 contains medium-scale, low-angle, cross-beds. The cross-sets are exemplified by the resistant nature of the lithic lapilli. The intracaldera facies contains several intervening air-fall tuff and surge deposits 4 to 10 m thick. The interbedded air-fall units are laterally continuous while the surge deposits are laterally discontinuous. Both of these intervening deposits thicken proximal to the vent complex.

Crystal content of the intracaldera facies is generally consistent, excluding surge deposits where gravity settling has concentrated the crystals. Phenocrysts are less than 3 mm and include 4 to 8 percent potassium feldspar, and 1 to 4 percent quartz.

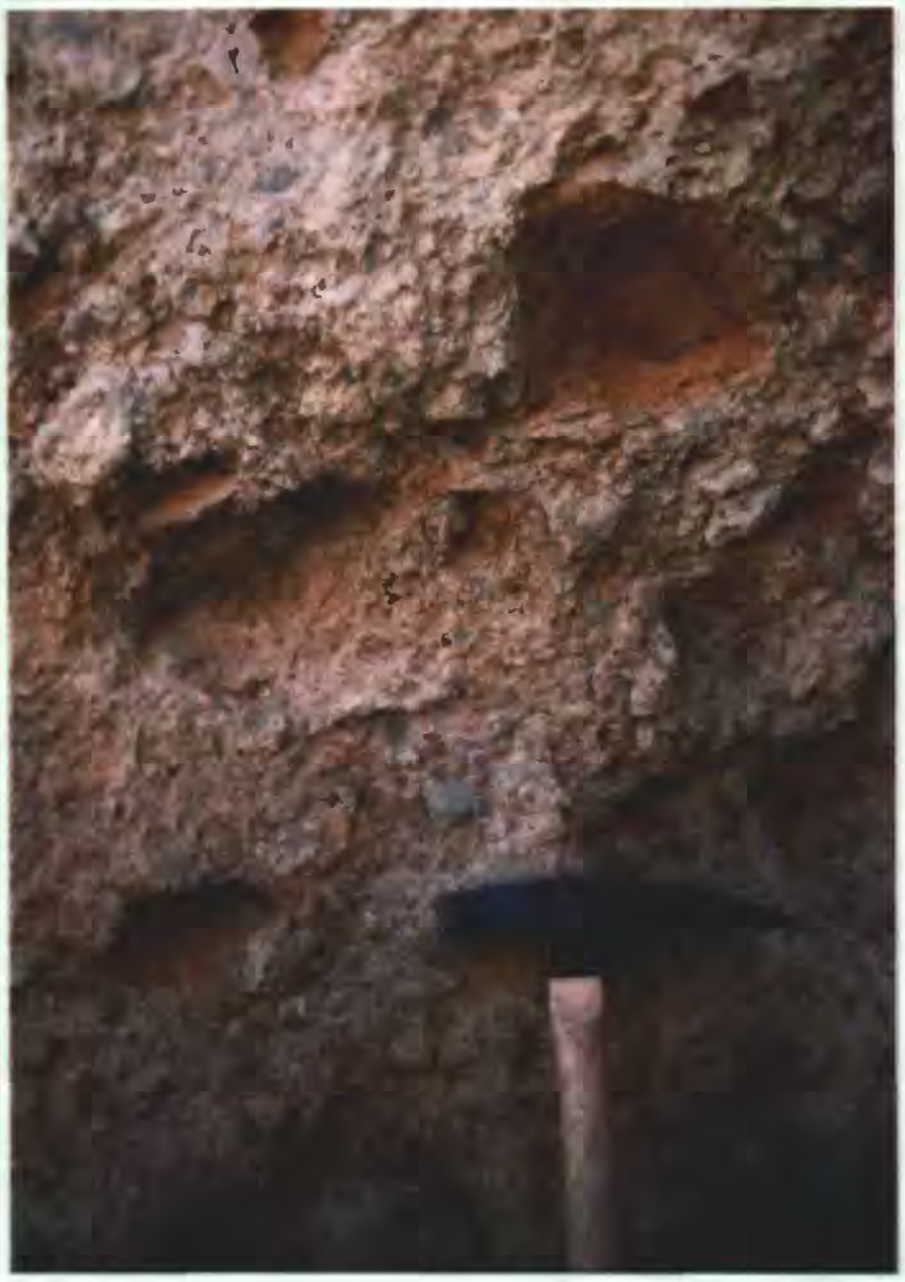

Figure 10. Near-vent intracaldera ash-flow tuff with orangish-brown pumice blocks and juvenile lithic fragments (magmatic inclusions). Pumice blocks greater than 10 cm across are common near the vent margin. Hammer head is 20 cm across.

Figure 11. Near-vent intracaldera ash-flow tuff with banded rhyolite block. Rhyolite blocks greater than 0.5 m across are common along the vent margin. Hammer is 40 cm long.

Figure 12. Medium-scale, low-angle, cross-beds within an ash-flow tuff of the intracaldera facies. Similar flow structures are illustrated in the measured section (Plate 2). Approximately 12 m of vertical section are shown in the photograph.

Air Fall Facies

The air fall facies is made up of bedded air-fall tuffs and interbedded ash-flow tuffs and surge deposits, all of which were deposited concurrently with the collapse of the Mahogany Mountain caldera. The unit has a minimum thickness of 200 m and covers approximately 45 km^2 within and adjacent to the caldera. Outside the caldera, the air fall facies stratigraphically overlies the outflow ash-flow tuff and is locally included with the outflow facies. Inside the the caldera, the air fall facies is separated from the underlying intracaldera facies by a gradational contact. Rocks stratigraphically above the contact are approximately 90 percent air-fall tuffs, while rocks below the contact are approximately 70 percent ash-flow tuffs. The stratigraphic section illustrated in plate 2, shows the gradational contact between air fall and intracaldera facies. For descriptive purposes the air fall facies is divided into lower and upper parts (fig. 7), both of which represent about half of the exposed section. The boundary between the lower and upper parts of the air fall facies is near the 1180 m stratigraphic elevation.

Lower Air Fall Facies. The lower part of the air fall facies is made up of nonwelded air-fall tuff, and several discontinuous interbedded partly welded ash-flow units and surge deposits. Angular unflattened orangish-brown pumice fragments and light green rhyolite lithic fragments (magmatic inclusions) are common throughout the lower air fall facies. Figure 13 shows a typical exposure of the bedded air-fall tuffs. Pumice fragments are usually altered to clays and form pitted features in the tuff. Lithic fragments have vesicular rims indicating they were molten when erupted. The pumice and juvenile lithic fragments are typically 1 to 3 cm in diameter, becoming larger and more abundant near the vent complex.

Oblong bombs and juvenile blocks of light green rhyolite are restricted to the lowermost part of the air fall facies. The bombs, blocks, and lithic fragments are unaltered and form positive relief on the erosional surface of the tuff (fig. 13). Angular blocks of brownish-grey banded rhyolite are randomly distributed throughout the lower part of the facies (fig. 14). These blocks are

Figure 13. Bedded air-fall tuff deposit typical of the Mahogany Mountain caldera. Layers of juvenile lithic fragments (magmatic inclusions) stand out against the less resistant lithic-poor ash layers. Approximately 1.5 m of vertical section shown in the photograph.

Figure 14. Near-vent bedded air-fall tuff with two large rhyolite blocks. The lower block has banded texture. Blocks greater than 0.5 m across are common along the vent margin. Hammer is 40 cm long.

typically altered to clays or are calcified. Texturally, the brownish-grey blocks appear identical to the rhyolite breccia that comprises the central-vent complex (following section). Blocks and bombs greater than 0.5 m across are common near the vent complex.

Upper Air Fall Facies. The upper part of the air fall facies consists predominantly of light brown to brownish-yellow reworked ash and air-fall tuff. Pumice and lithic fragments are smaller and less common in the upper part. Blocks and bombs are scarce or absent. The reworked ash locally contains abundant accretionary lapilli 0.3 to 2.5 cm in diameter. The accretionary lapilli contain concentric rings of fine ash, cored by green lithic fragments. The upper part of the air fall facies is generally less stratified than the lower part. The upper part consists of massive beds of ash with thin, discontinuous layers and stringers of pumice and lithic lapilli. Locally, the massive beds of ash are interrupted by layers of the reworked ash that contain sets of small-scale planar cross-lamina.

Discontinuous, lens-shaped beds containing sorted pumice and lithic fragments 3 to 8 cm in diameter are interstratified throughout the upper and lower air fall facies. The beds range from 5 to 15 m in length and 1 to 3 m in thickness (Plate 2). Freundt and Schmincke (1985) describe similar lithic units that were deposited in an alternating plinian-phreatomagmatic eruption at the Laacher See volcano, Germany. In that eruption, the lithic fragments segregated from pyroclastic flows primarily by gravitational setting and were deposited by a variety of topographic-controlled processes.

Crystals are scarce throughout the air fall facies. Phenocrysts are less than 2 mm, and include 1 to 4 percent potassium feldspar and quartz.

Vent Complex

Rhyolite plugs, dikes, and intrusive breccia form a 0.6- by 1.8-km irregular-shaped vent complex near the center of Mahogany Mountain caldera (fig. 5). The vent intrusions consist predominantly of matrix-supported autobreccia crosscut by dikes

and plugs of flow, and flow-foliated rhyolite. Along the north margin of the vent complex, the autobreccia locally intrudes and grades into the surrounding intracaldera tuffs. The east margin of the vent typically forms a sharp contact with the intracaldera tuff. Along this margin, large chaotic blocks of intracaldera tuff up to 10 m across reside within the vent breccia (fig. 4). Conversely, blocks of vent breccia up to 1.5 m across are contained within the adjacent intracaldera tuff. Eutaxitic structures or flow features are typically absent from the vent breccia; however, a crude vertical compression foliation is apparent adjacent to the rhyolite dikes.

Vent Breccia

The vent breccia consists of angular to subangular rhyolite fragments supported in a matrix of perlite and opaline silica. Color and texture of the breccia varies considerably throughout the vent complex due to devitrification, leaching, and clay alteration. Breccia fragments range from 0.5 to 20 cm in diameter; larger fragments are generally concentrated in the northern and central parts of the vent. Orangish-brown pumice fragments up to 15 cm across are locally concentrated in the vent breccia. Parts of the north vent consist exclusively of pumiceous breccia. The pumice fragments are usually altered to clays and form large pits and cavities in the breccia unit. These orangish-brown pumice fragments are texturally identical to those found in the adjoining ash-flow and air-fall tuffs. The vent breccia probably represents pyroclastic material that was deposited within the vent conduit during the last stages of explosive activity. Vents quenched at this stage, without any conduit closure, are briefly discussed by Wolff (1986).

Vesicle size and degree of vesiculation varies from place to place throughout the breccia unit. Vesiculation is attributed to many factors including: volatile content and silica saturation of the erupting magma, depth of emplacement, and size of the vent conduit. Post-emplacement alteration processes such as acid leaching may have contributed to the development of secondary vesicles as well as to the enlargement of primary vesicles.

Part of the vent breccia conformably intrudes bedded air-fall tuffs northeast of the vent complex (fig. 5), along Leslie Gulch Road. The sill varies from 8 to 12 m thick, extends 0.6 km

northeast along the road, and is approximately 120 m wide. At the margins of the sill, the air-fall tuff is densely welded due to secondary heating. Most of the sill is devitrified and consists of whitish-gray breccia fragments supported in a matrix of light green perlite (fig. 15). These breccia fragments do not contain vesicles. Isolated parts of the sill that are not devitrified consist of black glassy breccia fragments supported in a matrix of olive-green glass.

Phenocrysts are restricted to the breccia fragments. Phenocrysts are less than 4 mm, and include 1 to 3 percent sanidine and 1 to 2 percent quartz.

Rhyolite Dikes

At the surface, the vent breccia is intruded by a plug, five major dikes (fig. 5), and several smaller subsidiary dikes. Cross sections constructed through the vent complex (fig. 4) illustrate the intrusive relations between the plug, dikes, and vent breccia. The aphyric to slightly porphyritic rhyolite plug and dikes are pale brown to dark chocolate brown. They weather to pinnacles and spires, and contain well-developed flow folds, and high-angle to vertical sheet-banded flow foliation. Fold amplitudes range from 5 cm to 5 m across.

The slightly porphyritic rhyolites contain phenocrysts that are less than 3 mm. They include 2 to 4 percent potassium feldspar, 1 to 3 percent quartz, and less than 1 percent iron oxide.

Post-Caldera Ash-Flow Tuffs

Tuff of Spring Creek

The tuff of Spring Creek is a composite ash-flow tuff that erupted from the Three Fingers caldera. The caldera forms a north-trending 10- by 15-km topographic basin 4 km northeast of the Mahogany Mountain caldera (fig. 1). The tuff is exposed within the Mahogany Mountain caldera and north of the caldera (Plate 1), and covers an estimated 180 km^2. The tuff of Spring Creek consists of multiple ash flows less than 20 m thick that cooled as a single unit. Inside the Mahogany Mountain caldera, the ash-flow tuff forms a steep parallel unconformity with the

Figure 15. Intrusive autobreccia typical of the vent complex. This exposure is part of a sill that intrudes the north wall of Leslie Gulch Canyon. The angular to subangular rhyolite fragments are supported in a matrix of light green devitrified glass. Plastic scale is 15 cm long.

underlying caldera-forming ash-flow and air-fall tuffs (fig. 7). The tuff has a minimum thickness of 300 m where it fills the central graben of the caldera. The thickest section of the tuff is exposed along the southern topographic wall of the caldera. Here, it has a minimum thickness of 400 m.

The basal part of the tuff of Spring Creek consists of white to light green, partly welded, crystal rich ash-flow tuff. The basal part is less than 5 m thick and contains 20 to 25 percent quartz and feldspar phenocrysts. Stratigraphically above the crystal-rich basal zone, the rock is a light green partly welded ash-flow tuff. Purplish-brown to dark brown lithic fragments are randomly distributed throughout the tuff. Pumice fragments are usually medium green and stand out against a lighter green ash matrix. The vitric groundmass is composed of slightly distorted devitrified shards and unflattened to partly flattened pumice fragments. The tuff matrix locally displays mottled texture of whitish-green fine-grained ash enclosed in contrasting dark green coarse-grained ash matrix. Phenocrysts are less than 4 mm, and include 5 percent sanidine, 1 to 5 percent plagioclase (An_{10}), 1 to 2 percent quartz, and less than 1 percent soda pyroxene and iron titanium oxides.

In the Mahogany Mountain caldera, the upper 10 to 15 m of the tuff (fig. 7) contain numerous ellipsoidal, oblong, and spindle-shaped aphyric to slightly porphyritic basalt bombs. The bombs are typically clustered in small groups and range from 4 to 10 cm long. The bombs contain xenocrysts of quartz and sanidine that are encapsulated by reaction rims of microcrystalline pyroxene and amphibole. The basalt groundmass consists of microcrystalline plagioclase, olivine, and pyroxene. The tuff matrix contains large blocky sanidines 5 to 10 mm across. The sanidines comprise about 3 modal percent of the tuff. Percentage and size of plagioclase and quartz phenocrysts is unchanged from the lower to the upper parts of the tuff unit. Color and degree of welding is similar in both parts.

Tuff of Birch Creek

The tuff of Birch Creek probably vented from a source 15 to 25 km southwest of the Mahogany Mountain caldera. The tuff covers about 22 km^2 within the southern part of the caldera and along the Owyhee River west of the caldera (Plate 1). In the

Mahogany Mountain caldera, the thickness of the tuff ranges from 10 m in the southeast where it conformably overlies the tuff of Spring Creek, to approximately 40 m in the southwest where it unconformably overlies air fall facies of the Leslie Gulch Tuff. The tuff of Birch Creek is the youngest ash-flow tuff exposed in the caldera (fig. 7). The tuff thickens to an estimated 140 m in the Owyhee River Canyon, 10 km southwest of the caldera (Plate 1). Here, it laps against an angular unconformity developed on outflow facies of the Leslie Gulch Tuff (Plumley, 1986).

The tuff of Birch Creek is a light grayish-purple to grayish-brown nonwelded to welded rhyolite ash-flow tuff. The tuff consists of undistorted glass shards 0.5 to 1 mm long and sparse unflattened pumice fragments less than 5 cm across. Thicker sections of welded tuff that crop out in the western part of the caldera contain dark purplish-brown flattened pumice fragments up to 10 cm in length that stand out against a lighter ash matrix. The tuff has a well-developed eutaxitic foliation and contains 5 to 7 percent feldspar and quartz phenocrysts that are less than 4 mm across, and minor hornblende and biotite phenocrysts less than 2 mm across. The basal part of the ash-flow tuff is crystal rich and contains as much as 20 percent phenocrysts.

Rhyolite and Basalt Flows and Intrusions

Rhyolite Dikes

Three rhyolite dike systems intrude the Mahogany Mountain caldera and cut the entire sequence of intracaldera tuffs. Two of the rhyolite dike systems trend north across the length of the caldera, paralleling either side of the central graben (Plate 1). The third dike system trends northwest through the western part of the caldera and is broken by a series of en echelon faults. The rhyolite dikes are highly resistant to erosion and form steep spired ridges that rise 100's of meters above the intracaldera tuffs. Intracaldera tuffs adjacent to the rhyolite dikes are densely welded due to secondary heating. Hydrothermal alteration and silicification is common in parts of the dike system and in the adjoining tuff. Secondary welding and silicification of the adjoining tuffs further contributes to the resistant nature of the dikes.

The rhyolite dikes are 1 to 5 m thick and typically exhibit well-developed sets of horizontal columnar joints (fig. 16). Porphyritic rhyolite dikes are brownish-gray to brownish-silver and contain subequal amounts, 2 to 18 modal percent, of sanidine and quartz phenocrysts. Crystal size and percentage varies in different parts of a dike, and from dike to dike. The northwest-trending dike system that cuts the western part of the caldera contains sanidine phenocrysts as large as 10 mm, although most phenocrysts range from 2 to 5 mm. The rhyolite dikes also contain minor amounts of plagioclase (An_{10}), diopsidic-augite, biotite, and iron titanium oxide.

Rhyolite Ring-Domes and Flows

Domes and plugs of rhyolite porphyry intrude the northern and eastern margins of the Mahogany Mountain caldera (Plate 1). Flows and flow breccias of aphyric to slightly porphyritic rhyolite are associated with the larger intrusions. The plugs and domes form highly resistant knobs and craggy ridges that rise above the surrounding topography. Weathered surfaces exhibit vertical sheet flow foliation and large flow folds. Large blocks of rhyolite commonly exfoliate along these high-angle flow surfaces forming talus deposits at the base of the rhyolite protrusions. The larger plugs and domes are often capped by welded ash and lapilli tuffs. Hydrothermal alteration is common within and adjacent to the rhyolite intrusions. In the study area, the rhyolite intrusions are commonly dark grayish-red to brownish-gray and contain subequal amounts of of sanidine and quartz phenocrysts that range from 0.5 to 10 mm in diameter.

An extensive post-caldera rhyolite dome and flow complex intrudes sedimentary rocks along the eastern margin of the caldera. The rhyolite complex occupies Bannock Ridge and covers approximately 14 km^2. Cross section B-B' (Plate 1) illustrates the structural and stratigraphic relation between the rhyolite intrusion and the caldera margin. The basal part of the complex, exposed along the southwest flank of Bannock Ridge, consists of 50 to 80 m of light green to tan brown ash, and lapilli air-fall tuff. Stratigraphically above the air-fall tuff, layers of grayish-black vitrophyre are interstratified with aphyric to slightly porphyritic

Figure 16. Rhyolite dike exposed along the northeastern margin of the Mahogany Mountain caldera. Horizontal columns indicate primary cooling occurred from the dike walls. Hammer is 40 cm long. Basin in the far left background is the topographic expression of the Three Fingers caldera.

reddish-brown rhyolite. The vitrophyre layers probably represent cooling breaks in a rhyolite flow sequence. Near the center of Bannock Ridge, the rhyolite flows are an estimated 220 m thick, thinning towards the flanks (Plate 1). The middle and upper parts of the rhyolite sequence are locally fold and flow foliated, and have abundant vapor-phase cavities. Phenocrysts range from 1 to 3 mm, and include 1 to 5 percent potassium feldspar and quartz, in a devitrified groundmass.

Massive beds of rhyolite lithic breccia and flow breccia are exposed along the northern part of Bannock Ridge and are locally included with the Bannock Ridge rhyolite complex (Plate 1). Lithic fragments are generally less than 14 cm across. Flank and distal units of the rhyolite complex are typically composed of homogeneous flow breccias that have maximum flow distances of 3 to 4 km. Phenocryst assemblages are similar to those of the main dome-forming flows.

Basalt Flows and Shallow Intrusions

Plateau-forming basalt flows cover approximately 6 km^2 within the western part of the caldera (Plate 1). The dense aphyric to porphyritic tholeiitic basalt flows are commonly columnar jointed and locally contain basal flow breccias. The flows are typically 12 to 24 m thick. In the caldera, basalt dikes, sills, and plugs intrude all of caldera-forming and post-caldera tuffs. The most extensive basalt intrusions are exposed in the west-central part of the caldera along the Owyhee Reservoir. A closed gravity low (B; fig. 6) is centered over these intrusions.

Phyric basalt textures range from hyaloophitic to intergranular. Phenocrysts include 1 to 6 percent plagioclase (An_{45-60}) as large as 6 mm, 1 to 4 percent clinopyroxene, and minor olivine, orthopyroxene, and iron oxides.

Sedimentary Rocks

Isolated outcrops of lacustrine sedimentary rocks are exposed in the northeastern part of the caldera. These rocks unconformably overlie the post-caldera tuffs and have a maximum thickness of 37 m. The lacustrine sedimentary rocks consist of fine-bedded tuffaceous sandstone, siltstone, and mudstone. Along

the northeast topographic wall of the caldera, the sedimentary rocks are locally silicified and altered with zeolite minerals.

An estimated 400 m of post-caldera fluvial and lacustrine sedimentary rocks fill the western part of the caldera. The thickest section of sedimentary rock is exposed within a north-trending graben (Plate 1). These rocks include; beds of arkosic sandstone 1 to 3 m thick, beds of reworked pyroclastics 10 to 20 m thick, and massive beds of tuffaceous siltstone and mudstone 20 to 30 m thick that contain interbeds of diatomaceous earth 1 cm to 1 m thick. The moderately indurated, coarse-grained, arkosic sandstones contain small-scale, high-angle, planar cross-beds. The beds of reworked pyroclastics contain medium-scale, low-angle, trough cross-beds.

Bedded Maar deposits consisting of ash, basaltic pumice lapilli, and basalt blocks are also exposed in the western part of the caldera. The deposits are intercalated with sedimentary rocks and have a maximum thickness of 25 m.

GEOCHEMISTRY

Sampling and Analytical Method

Bulk samples of the intracaldera ash-flow and air-fall tuff were collected from three measured sections and several stratigraphic horizons around the vent complex. Bulk samples of the vent breccia were collected along the length, width, and depth of the vent complex. Most of the bulk samples used for the chemical analyses contained retrievable pumice fragments and juvenile lithic fragments (magmatic inclusions). Unaltered pumice fragments and magmatic inclusions were separated from the bulk samples and analyzed independently. Chemical data gathered from the separates represent preeruptive magma compositions.

Pumice separates were retrieved by carefully scraping pumice lumps from the samples. Inclusion separates were retrieved by simply breaking out the resistant fragments, then scraping to remove any ash and pumice matrix.

Nineteen bulk rock samples, 1 pumice separate, and 1 magmatic inclusion were analyzed for the major-elements Si, Al, Fe, Mg, Ca, Na, K, Ti, P, and Mn. Five of the bulk samples were collected from the intracaldera ash-flow tuff, 9 from the air-fall tuff, and 5 from the vent intrusion. The major-elements were analyzed by direct current arc spectroscopy and are presented in table 1. Major-element analyses were completed by the U.S. Geological Survey, Branch of Analytical Chemistry. Percentages are calculated to water-free values to help re-establish relative amounts of major-elements lost during weathering.

Twenty-eight bulk samples, 11 pumice separates, and 5 magmatic inclusions were analyzed for the trace-elements Sr, Rb, Y, Zr, and Nb, and an additional 25 samples were analyzed for the trace-elements Ba, La, Ce, and Zn. Eleven of the bulk samples were collected from the intracaldera ash-flow tuff, 10 from the air-fall tuff, and 7 from the vent intrusion. To avoid contamination during preparation, all rocks were ground in an agate mortar and sieved through mylar screens. Trace-element abundances were analyzed on pressed powder pellets by X-ray fluorescence spectroscopy and are presented in table 2.

Table 1. Major-element analyses of Leslie Gulch intracaldera ash-flow tuff (Tlgi), air-fall tuff (Tlga), and vent intrusion (Trvi) from the Mahogany Mountain caldera. Analyzed by direct current arc spectroscopy, presented as weight percent of oxides, and calculated to water free values.

	Sample no.	Unit	SiO_2	Al_2O_3	$FeTO_3$	MgO	CaO	Na_2O	K_2O	TiO_2	P_2O_3	MnO	Total
1	VM-59-85	Tlgi	70.1	13.4	2.86	<0.2	0.81	7.6	3.25	0.21	0.02	0.14	98.6
2	VM-66-85	Tlgi	71.9	13.1	2.94	<0.2	0.84	4.5	4.16	0.22	0.04	0.07	97.9
3	VM-73-85	Tlgi	73.4	12.7	3.20	<0.2	0.50	3.9	5.11	0.28	0.02	0.05	99.4
4	VM-85-85	Tlgi	69.8	13.7	4.04	0.68	2.65	3.7	3.65	0.44	0.13	0.07	98.9
5	VM-93-85	Tlgi	73.7	12.4	2.92	<0.2	0.57	3.7	5.34	0.25	0.04	0.06	98.8
6	VM-91P-85	Tlgi	64.8	16.1	3.37	<0.2	0.64	1.6	12.58	0.28	<0.02	0.18	99.8
7	CO-37-84	Tlga	77.9	10.2	1.58	0.48	0.58	0.27	8.29	0.18	0.09	<0.02	99.6
8	VM-29-85	Tlga	74.7	12.2	2.99	<0.2	0.66	3.9	4.18	0.26	0.04	0.06	99.2
9	SO-38-84	Tlga	67.3	14.7	2.83	1.12	1.89	3.4	8.03	0.21	<0.05	0.02	99.6
10	VM-46-85	Tlga	76.7	11.2	2.67	<0.2	0.54	2.8	5.34	0.23	<0.02	0.05	99.8
11	VM-40I-85	Tlga	81.7	7.70	1.72	<0.2	0.65	1.7	5.24	0.17	0.04	0.03	99.2
12	VM-62-84	Tlga	76.2	11.0	2.26	0.46	0.22	3.4	5.60	0.18	<0.05	0.02	99.4
13	VM-80-85	Tlga	68.4	14.1	3.27	<0.2	3.52	3.9	5.14	0.33	0.04	0.08	99.0
14	VM-129-84	Tlga	75.9	11.3	2.22	0.26	1.70	3.7	4.42	0.16	<0.05	0.03	99.7
15	VM-137-84	Tlga	74.9	12.3	2.80	0.18	0.03	4.0	4.59	0.22	<0.05	0.03	99.1
16	VM-143-84	Tlga	75.9	11.7	2.34	0.35	0.19	3.6	4.48	0.19	<0.05	0.03	98.8
17	VM-24-85	Trvi	75.3	12.1	2.36	<0.2	0.26	3.3	5.59	0.22	0.02	0.02	99.4
18	VM-26-85	Trvi	73.5	12.9	2.86	<0.2	0.29	2.9	6.83	0.27	0.02	0.05	99.8
19	VM-45-85	Trvi	75.6	12.0	2.59	<0.2	0.91	4.3	3.43	0.23	<0.02	0.05	99.3
20	VM-45A-85	Trvi	74.7	12.5	3.03	<0.2	0.83	3.9	4.45	0.27	0.04	0.05	99.9
21	VM-98-85	Trvi	74.9	12.2	2.65	<0.2	0.28	3.8	4.89	0.23	0.02	0.04	99.2

Table 2. Representative trace-element analyses of Leslie Gulch intracaldera ash-flow tuff (Tlgi), air-fall tuff (Tlga), and vent intrusion (Trvi) from the Mahogany Mountain caldera. Trace-elements analyzed by X-ray fluorescence spectroscopy, presented in ppm. Unavailable data represented by (*).

	Sample no.	Separate	Unit	Rb	Sr	Y	Zr	Nb	Ba	La	Ce	Zn
1	VM-35-85		Tlgi	97	10	91	634	32	*	*	*	*
2	VM-35I-85	inclusion	Tlgi	95	36	53	239	7	*	*	*	*
3	VM-37-85		Tlgi	92	10	106	671	38	*	*	*	*
4	VM-37P-85	pumice	Tlgi	161	14	145	768	38	*	*	*	*
5	VM-59-85		Tlgi	94	10	126	610	38	660	92	178	395
6	VM-57P-85	pumice	Tlgi	440	8	249	1214	79	*	*	*	*
7	VM-65-84		Tlgi	151	26	109	679	41	883	22	45	241
8	VM-65P-84	pumice	Tlgi	68	269	303	1589	110	2285	283	454	603
9	VM-66-85		Tlgi	98	18	124	680	40	850	100	162	230
10	VM-69-85		Tlgi	97	11	108	595	37	*	*	*	*
11	VM-71P-85	pumice	Tlgi	128	22	200	1284	52	*	*	*	*
12	VM-70I-85	inclusion	Tlgi	62	24	182	423	26	*	*	*	*
13	VM-73-85		Tlgi	124	12	130	750	48	1100	100	174	225
14	VM-85-85		Tlgi	110	106	48	325	22	1100	46	72	100
15	VM-93-85		Tlgi	168	16	146	660	48	1000	130	180	230
16	VM-91P-85	pumice	Tlgi	450	32	176	830	54	2400	134	192	250
17	VM-101-85		Tlgi	152	9	136	680	40	*	*	*	*
18	VM-100P-85	pumice	Tlgi	340	60	736	4232	163	*	*	*	*
19	VM-116-85		Tlgi	141	13	136	784	44	*	*	*	*
20	VM-116P-85	pumice	Tlgi	301	46	211	1147	68	*	*	*	*

Table 2. (continued)

	Sample no.	Separate	Unit	Rb	Sr	Y	Zr	Nb	Ba	La	Ce	Zn
21	CO-37-84		Tlga	98	37	51	389	23	784	43	72	*
22	VM-29-85		Tlga	124	28	106	620	38	1500	96	146	176
23	VM-31-85		Tlga	125	17	97	655	39	*	*	*	*
24	VM-31I-85	inclusion	Tlga	81	11	49	381	24	*	*	*	*
25	SO-38-84		Tlga	215	82	150	880	60	207	104	172	225
26	VM-46-85		Tlga	140	24	106	590	40	970	104	166	198
27	VM-46P-85	pumice	Tlga	65	124	389	1284	85	*	*	*	*
28	VM-40I-85	inclusion	Tlga	102	10	70	390	30	720	68	110	136
29	VM-62-84		Tlga	97	23	102	668	50	730	108	182	225
30	VM-80-85		Tlga	136	34	116	720	48	1400	104	164	166
31	VM-129-84		Tlga	67	24	49	382	16	632	49	77	116
32	VM-137-84		Tlga	124	23	118	650	46	914	121	206	181
33	VM-143-84		Tlga	104	24	110	661	43	941	119	184	234
34	VM-11-85		Trvi	152	7	125	610	38	*	*	*	*
35	VM-11P-85	pumice	Trvi	209	22	152	973	57	*	*	*	*
36	VM-11I-85	inclusion	Trvi	81	8	94	576	33	*	*	*	*
37	VM-24-85		Trvi	150	10	110	640	46	96	110	164	190
38	VM-26-85		Trvi	154	10	108	680	44	890	86	168	205
39	VM-26P-85	pumice	Trvi	209	10	113	758	47	*	*	*	*
40	VM-45-85		Trvi	180	10	110	610	38	890	80	150	188
41	VM-45A-85		Trvi	148	10	114	620	38	880	112	172	215
42	VM-55-85		Trvi	134	10	116	610	42	830	90	150	215
43	VM-55P-85	pumice	Trvi	110	10	120	660	44	790	112	182	225
44	VM-98-85		Trvi	146	12	130	660	42	920	118	170	188

Analytical Data

The intracaldera ash-flow and air-fall tuffs and vent intrusion of the Mahogany Mountain caldera are peralkaline rhyolite. Based on Macdonald's (1974) classification of peralkaline silicic rocks (fig. 17) the intracaldera tuffs range from comendite to comenditic trachyte. Most of the analyzed rocks are either hydrated or crystalline. Soda loss is typical during hydration and recrystalization of peralkaline tuffs (Noble, 1970; Leat and others, 1984). Effects of these chemical processes can cause a loss of up to half the original Na_2O content. Widespread alteration of the feldspars in the intracaldera tuffs and vent intrusion prohibit the use of Rb and Sr as a correlation tool. The incompatible trace-elements Nb, Y, and Zr are less susceptible to alteration, and are useful in correlating some of the partly altered rocks in and near the vent intrusion.

The intracaldera tuffs show a large range in major-element compositions (Table 1). SiO_2 ranges from 81.7 to 64.8 percent, and Al_2O_3 ranges from 16.1 to 7.7 percent. The large range of major-element compositions is accompanied by a strong trace-element gradient. The most striking gradients are detected in the incompatible suite, with Zr ranging from 325 to 4232 ppm, Nb 7 to 163 ppm, and Y 48 to 736 ppm (Table 2). The elevated abundances of the incompatible trace-elements are characteristic of silicic peralkaline rocks, and are comparable to pantellerites (Noble and others, 1974). Rocks with similar Zr abundances are described by Mahood and Hildreth (1986) at the peralkaline volcano of Pantelleria.

Two compositions are distinguished among the intracaldera erupted products of the Mahogany Mountain caldera. The compositions include, (1) intermediate-silica comendite to comenditic trachyte enriched with Al, Fe, K, Y, Zr, Nb, Ba, and Zn, and (2) high-silica comendite depleted in Y, Zr, Nb, La, and Ce. These contrasting compositions represent a high-silica/ intermediate-silica bimodal magmatic system. The extreme depletion in Zr, Nb, and Y is unusual for a high-silica melt. Conversely, extreme enrichment in Zr, Nb, and Y seems

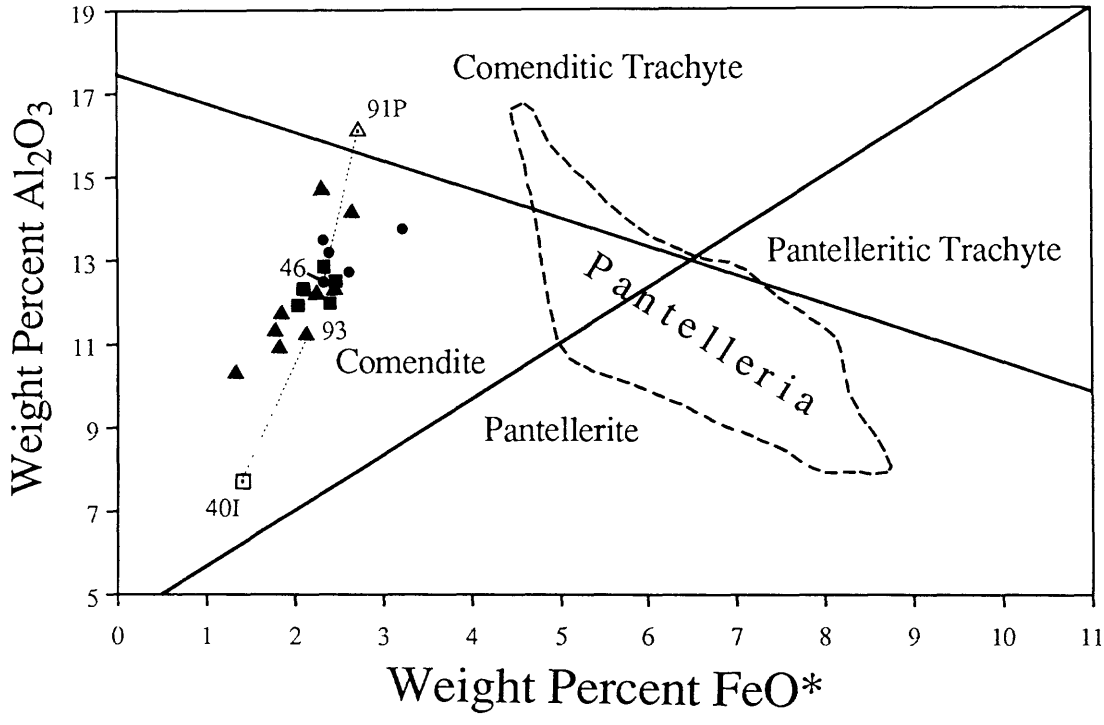

Figure 17. Intracaldera tuffs and intrusions of the the Mahogany Mountain caldera plotted in Macdonald's (1974) classificatory scheme for peralkaline extrusive rocks, based on Al_2O_3 versus total iron (FeO*). Symbols: solid circle, ash-flow tuff; solid triangle, air-fall tuff; solid square, vent intrusion; open triangle, pumice separate; open square, lithic separate. Dotted line connects separates with their parent bulk samples. For comparison, dashed line shows field of pantellerites from pantelleria (Macdonald and Bailey, 1973).

uncharacteristic high for a intermediate-silica melt. Magmatic systems with these characteristics have not been reported.

Major- and Trace-Element Composition

Major-Element Content

Abundances of SiO_2 and Al_2O_3 for 19 bulk samples and 2 separates are presented in figure 18. Major-element data indicate a large compositional gap exists in the intracaldera ash-flow and air-fall tuffs of the Mahogany Mountain caldera. Bulk samples of the tuffs and vent intrusion (37 and 38; fig. 18) range from a slightly oversaturated 78 percent SiO_2 to an intermediate 67 percent. Most of the bulk samples plotted on figure 18 range from 75 to 77 percent SiO_2.

In figure 18, the lower end of the trend is established by 2 pumice-rich bulk samples (solid triangles), and a pumice separate (open triangle). Of the 21 samples analyzed, these three samples (80, 38, and 91P; fig. 18) have the lowest detected SiO_2 values. Conversely, the upper end of the trend is established by a bulk sample that contains abundant magmatic inclusions, and a magmatic inclusion separate (37 and 40I; fig. 18). Both of these samples are oversaturated with SiO_2.

Natural sorting that occurred in the air falls produced pumice rich layers and layers containing high concentrations of magmatic inclusions (fig. 13). Bulk samples collected and analyzed from these sorted horizons plot on their respective ends of the silicic trend. Bulk samples collected from pumiceous layers plot at the low end of the trend, and bulk samples collected from inclusion-rich horizons plot at the upper end of the trend (solid triangles; fig. 18). A continuous range of silica compositions is not apparent. Natural mixing of the pyroclastic fragments produced the range of compositions. This range is represented simply as well-mixed bulk samples. These field relations and analytical data suggest that a sharp compositional transition zone existed in the magma chamber prior to eruption. The magmatic inclusions represent a high-silica melt in the upper part the chamber, and the pumice fragments represent an underlying intermediate-silica melt. Other magmatic systems that contained rhyolite and zoned

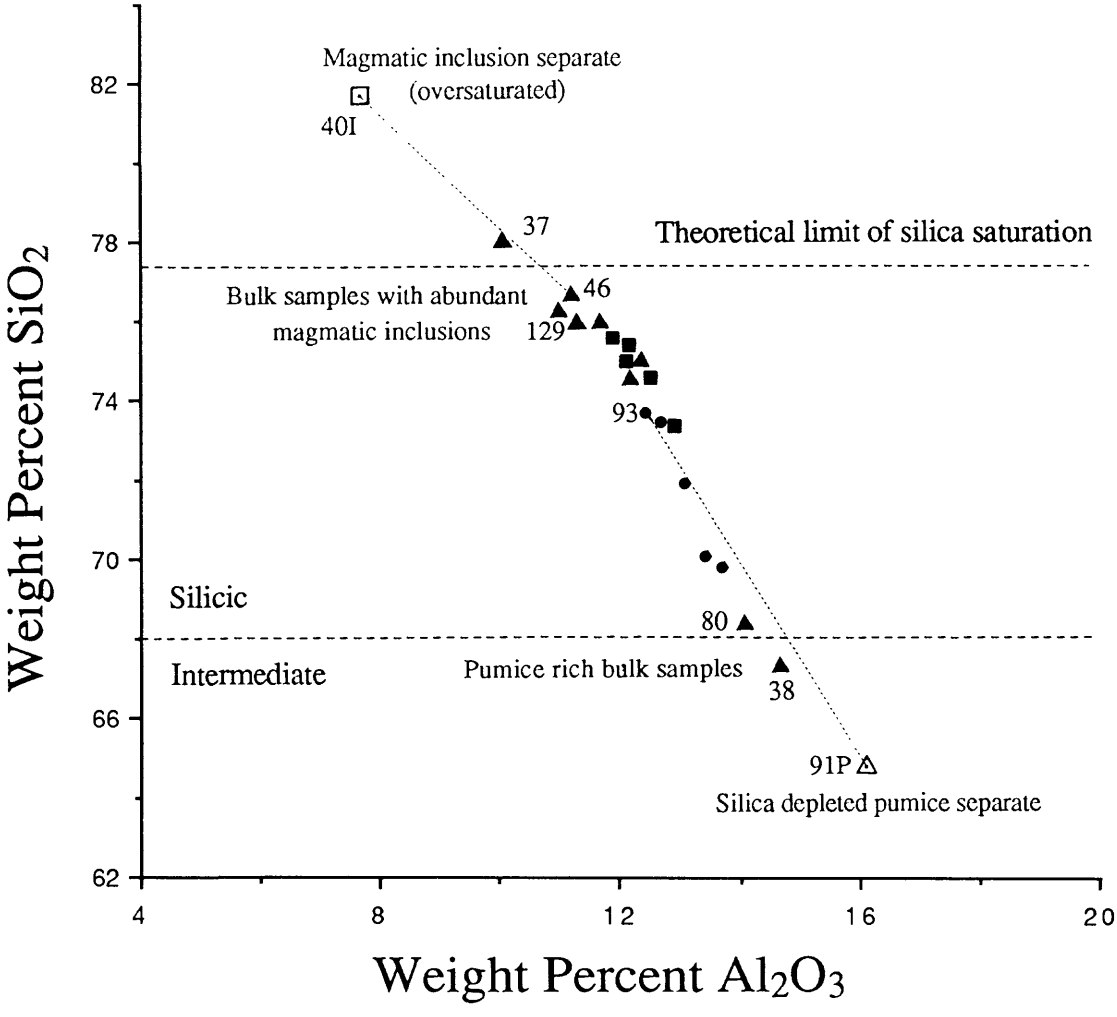

Figure 18. SiO_2 versus Al_2O_3 for samples of intracaldera ash-flow and air-fall tuff, and vent intrusion. Numbered samples are discussed in the text. Symbols: solid circle, ash-flow tuff; solid triangle, air-fall tuff; solid square, vent intrusion; open triangle, pumice separate; open square, magmatic inclusion separate. Dotted lines connect separates with their parent bulk samples.

intermediate melts with large compositional gaps are described by Hildreth (1981).

Trace-Element Content

Abundances of Nb and Zr (Table 2) are plotted against each other in five variation diagrams (fig. 19a,b,c,d, and e) to show similarities between the intracaldera tuffs and vent intrusion. Nb and Zr are used in these diagrams because of their wide range (325 to 4232 ppm and 7 to 163 ppm, respectively), and because of their high solubility in peralkaline melts (Watson, 1979; Mahood and Hildreth, 1983).

Abundances of Nb and Zr are plotted in figure 19a for the same bulk samples and separates shown in figure 18. The diagrams show the relation between trace-element data and whole rock data. Two striking similarities appear in the major-and trace-element variation diagrams, they are; (1) pumice fragments and magmatic inclusions plot at either end of the trend, suggesting that they represent compositional extremes, and (2) most of the bulk samples plot in a central cluster that represents an average composition. As discused for figure 18, natural sorting of the pyroclastic fragments produced compositional differences in the tuffs. Bulk samples collected and analyzed from these sorted horizons plot on their respective ends of the trend (fig. 19a). Average trace-element abundances are represented by well-mixed bulk samples.

The lower end of the trend is established by 3 bulk samples and a magmatic inclusion separate (129, 37, and 40I; fig. 19a). These samples are high-silica comendite (fig. 17) that contain the lowest detected concentrations of incompatible trace-elements of the intracaldera tuffs. The upper end of the trend is established by two pumice-rich bulk samples and a pumice separate (80, 38, and 91P; fig. 19a). The pumiceous samples are intermediate-silica comendite- to comenditic-trachyte (fig. 17), and contain extremely high concentrations of the incompatible trace-elements Nb, Zr, and Y. The pumice and magmatic inclusion end members established by trace-element data in figure 19a, suggests that a large compositional gap existed in the magma chamber prior to eruption.

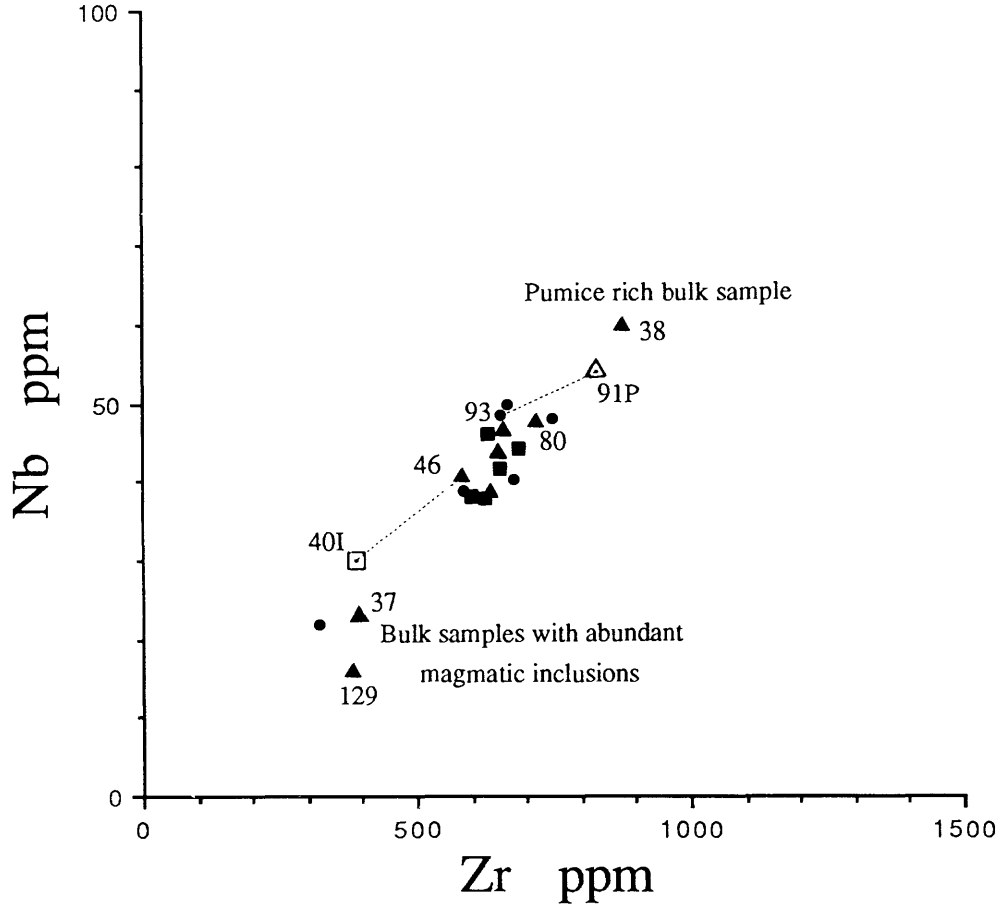

Figure 19a. Nb versus Zr for samples of intracaldera ash-flow and air-fall tuff, and vent intrusion. Numbered samples are discussed in the text. Symbols as in figure 18. Dotted lines connect separates with their parent bulk samples.

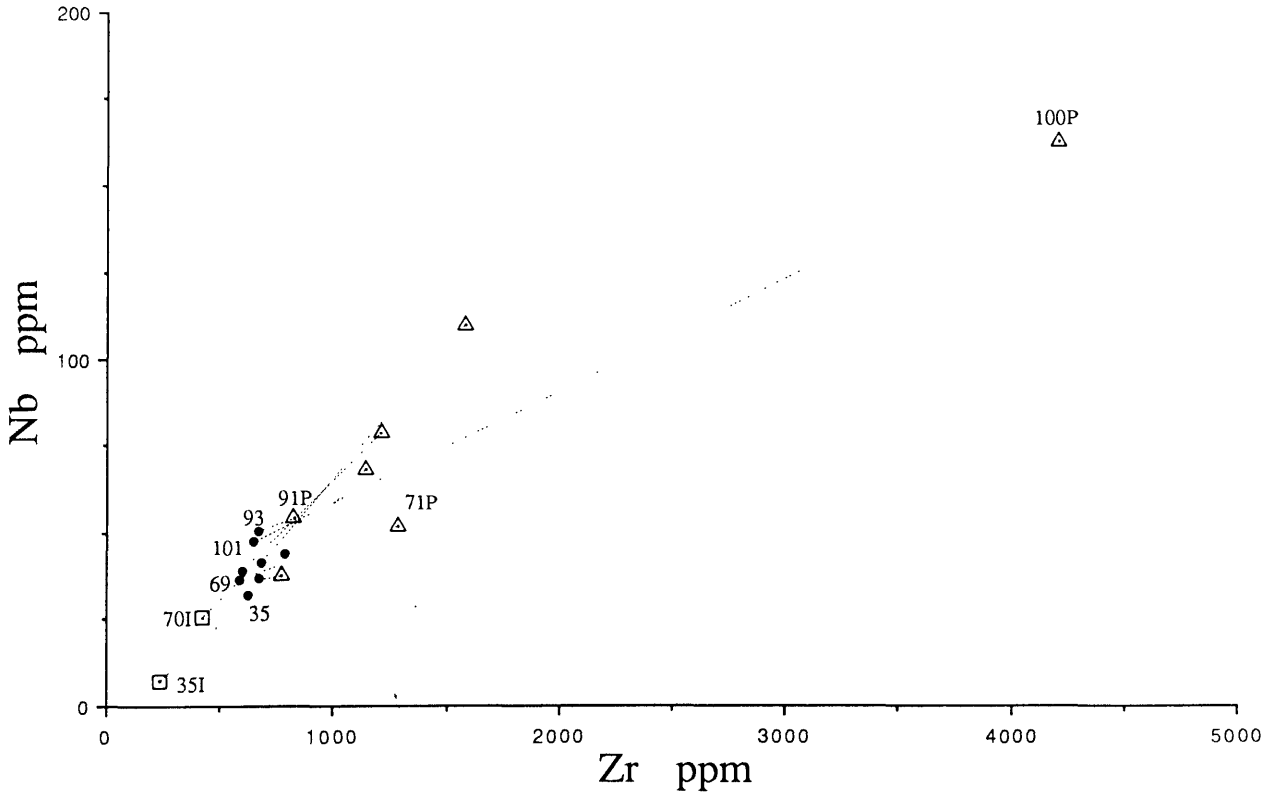

Figure 19b. Nb versus Zr for samples of intracaldera ash-flow tuff. Symbols: solid circle, ash-flow tuff; open triangle, pumice separate; open square, magmatic inclusion separate.

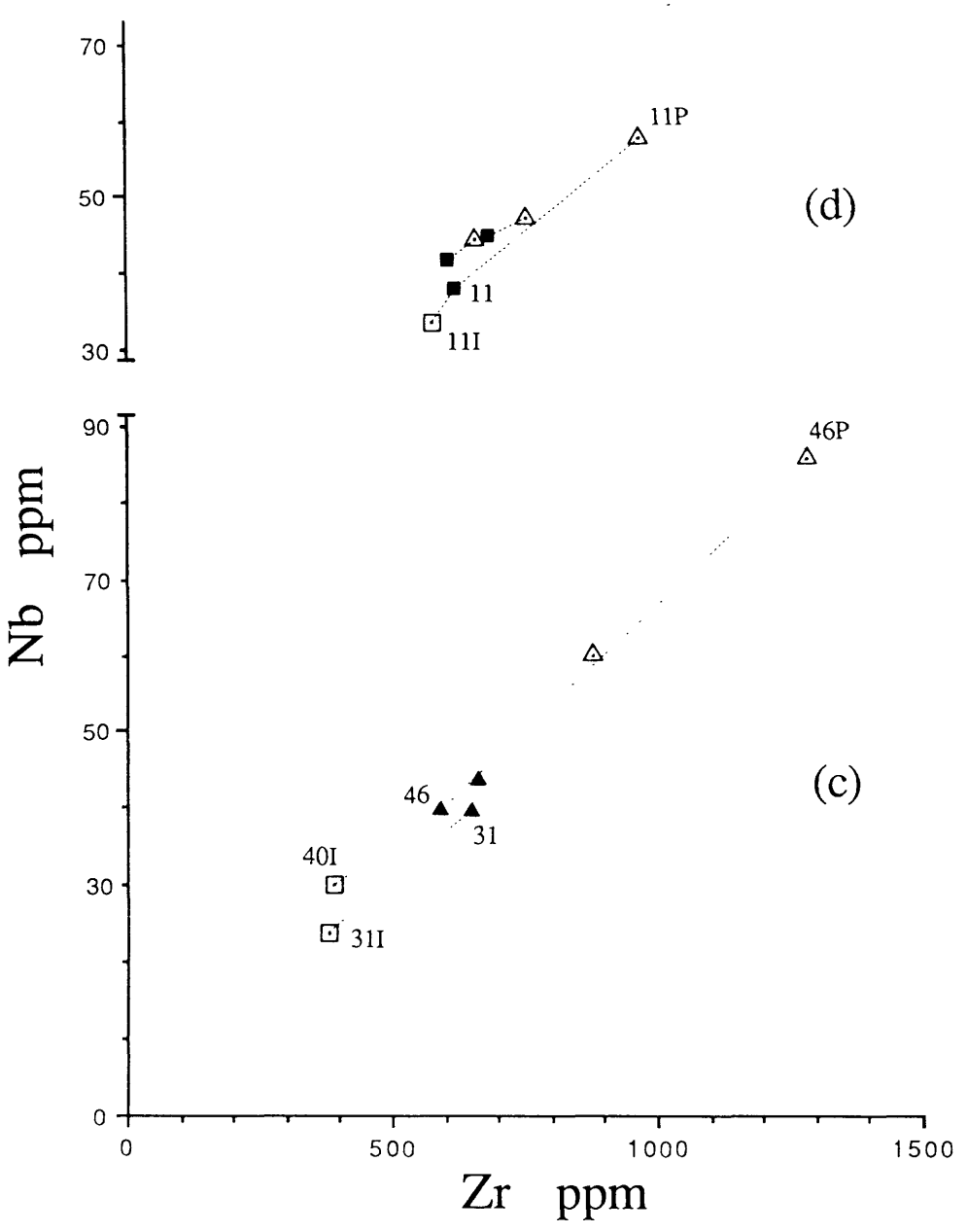

Figure 19c and 19d. Nb versus Zr for samples of intracaldera air-fall tuff (c) and vent intrusion (d). Symbols: solid triangle, air-fall tuff; solid square, vent intrusion, open triangle, pumice separate; open square, magmatic inclusion separate. Dotted lines connect separates with their parent bulk samples.

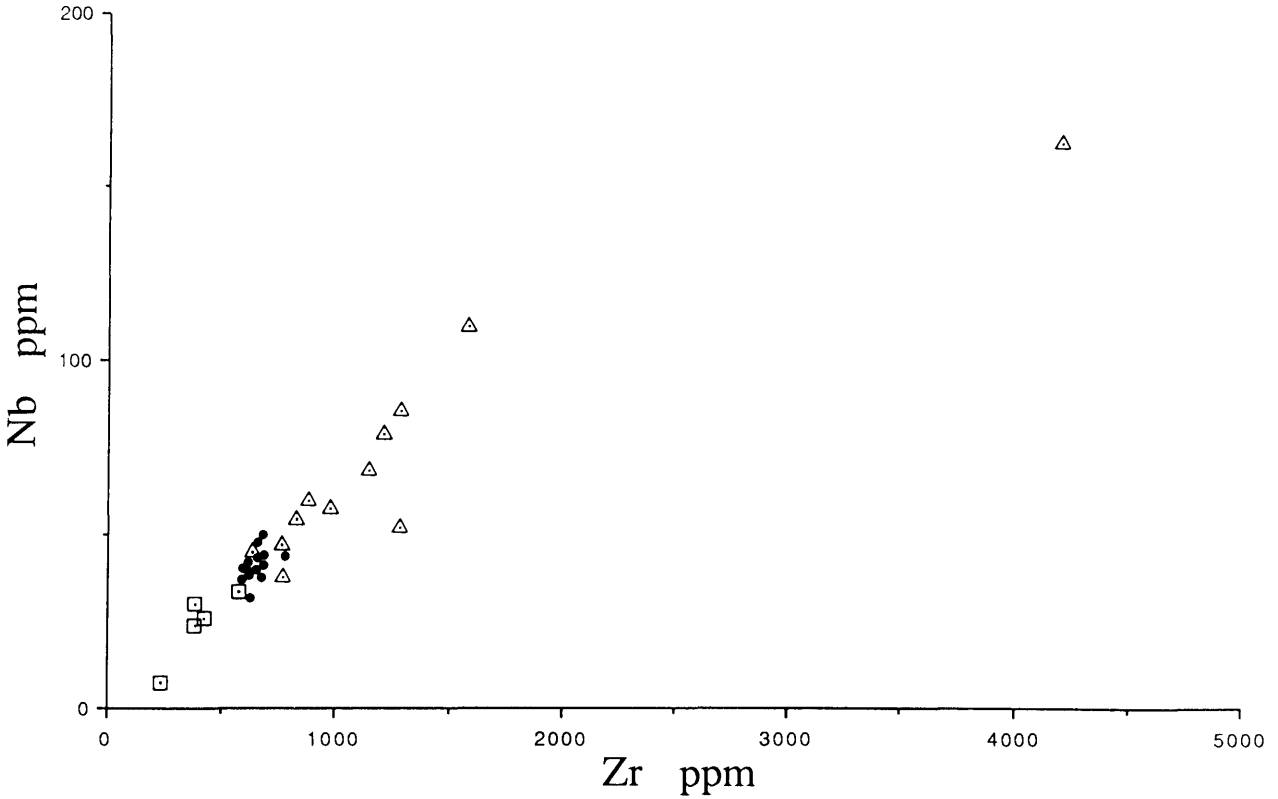

Figure 19e. Nb versus Zr for all samples of intracaldera tuff, and vent intrusion. Symbols: solid circle, all tuffs and vent intrusion; open triangle, pumice separate; open square, magmatic inclusion separate.

Trace-element Gradient

Variation diagrams (fig. 19b,c, and d) illustrate the abundances of Nb and Zr for each of the main units in the Mahogany Mountain caldera. These data show that the intracaldera ash-flow and air-fall tuffs, and vent intrusion have similar trace-element compositional trends. Each unit contains pumice separates enriched with Nb and Zr, magmatic inclusion separates depleted with Nb and Zr, and bulk samples that generally reflect an average composition. As observed in figures 18 and 19a, pumice fragments and magmatic inclusions collected from the intracaldera units represent opposing compositional end members. These consistent similarities suggest that the intracaldera tuffs and vent intrusion are comagmatic.

Figure 19e is a variation diagram that combines Nb and Zr data from all of the bulk samples and separates. The diagram shows the compositional consistencies that exist between the intracaldera tuffs and vent intrusion. An extraordinary wide compositional gradient exists in the pumice separate data, ranging from 660 to 4232 ppm Zr, and 44 to 163 ppm Nb. The pumice component represents the intermediate melt that occupied the magma chamber. The highest values are detected in the ash-flow tuff (fig. 19b) which erupted first. The lowest values are detected in the vent intrusion (fig. 19d) which erupted last. These data suggest the eruption tapped a intermediate-silica magma that had a steep trace-element compositional gradient.

Discussion of Magma Chamber Model

A two-component magma chamber with a large compositional gap is proposed for the Mahogany Mountain caldera. A schematic representation of the magma chamber is illustrated in figure 20. The chamber contains a high-silica peralkaline cap and an underlying intermediate melt. Density and thermal differences between these two melts probably inhibited mixing across a compositional interface (fig. 20).

High-silica peralkaline caps are typically enriched with incompatible trace-elements, certain rare earth elements (REE's), and halogens (Rytuba, 1981). Roofward enrichment in

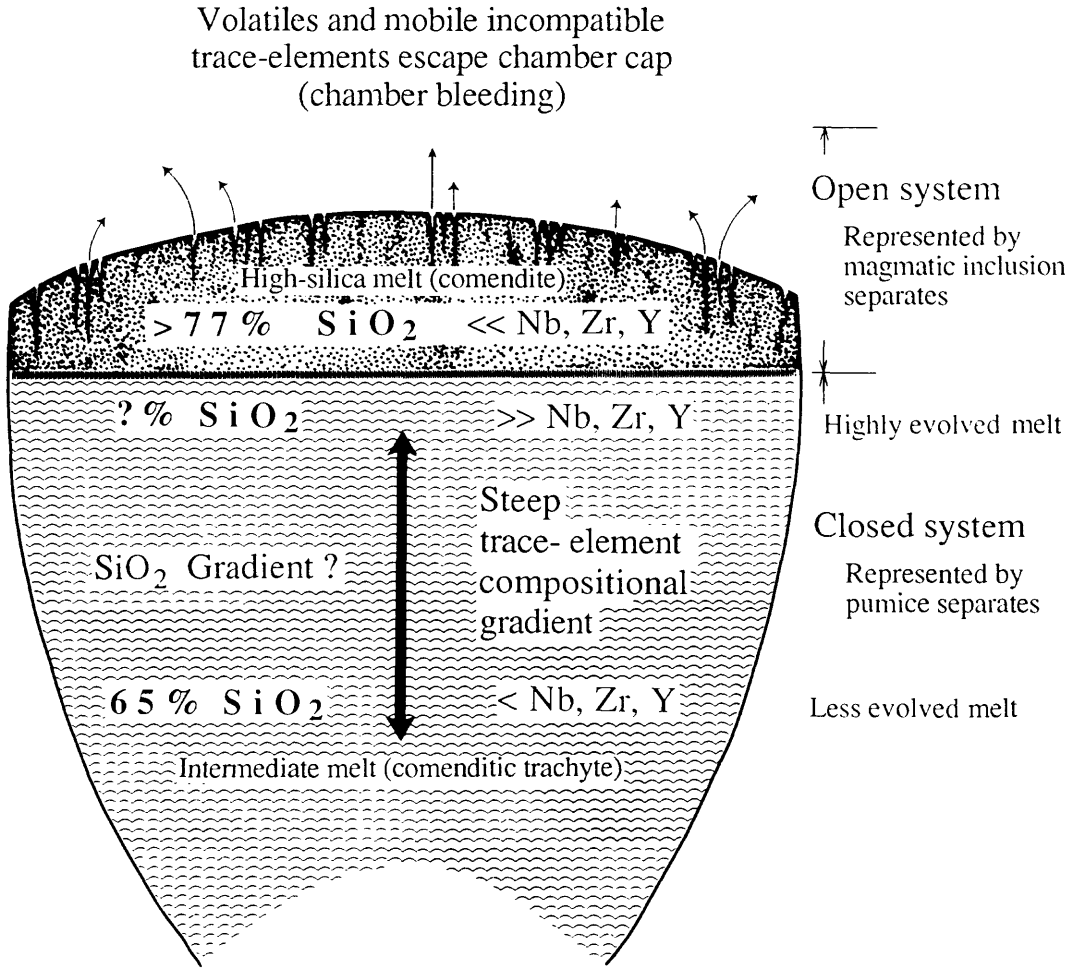

Figure 20. Schematic model of the Mahogany Mountain caldera magmatic system, as discussed in the text. The high-silica cap is an open system that releases volatiles and certain incompatible trace-elements. The underlying melt is a closed system that retains a compositional gradient.

incompatible trace-elements may be linked to roofward enrichment in the volatiles. Elements that are free to combine and move with the volatiles migrate roofward as volatile complexes (Mahood, 1981). The chamber cap depicted in figure 20 is an open system that is actively releasing its volatiles by a process known as "chamber bleeding". By this process, the otherwise silica-enriched cap is severely depleted of its volatiles and mobile trace-elements. Swanson and Walker (1988) have documented episodic volatile releases from a highly evolved silicic magma. In that system, a series of vapor releases and build-ups was followed by a final release that quenched the system.

The upper part of the magma chamber (fig. 20) is an open system that may have periodically developed a gradient. High-silica magmatic inclusions that contain low concentrations of incompatible trace-elements are representative of this system. These inclusions make up an estimated 30 to 40 percent of the intracaldera tuffs and vent intrusion.

The lower part of the magma chamber illustrated in figure 20 is a closed system that retained volatiles and developed a compositional gradient. The intermediate-silica pumice separates enriched with incompatible trace-elements are representative of this system. The compositional gradient that developed here is reflected in the trace-element data obtained from the pumice fragments (fig. 19b,c, and d).

Figure 21 is a cartoon sketch of the Mahogany Mountain caldera illustrating the caldera-forming central-vent eruption. Caldera-forming eruptions typically empty about 10 percent of their underlying magma chamber (Smith, 1979). This estimate is based upon the chemical variation and eruptive mechanism of zoned silicic systems, such as the Valles caldera, New Mexico, Timber Mountain caldera complex, Nevada, and the San Juan volcanic field, Colorado. During the Mahogany Mountain caldera eruption, the upper part of the closed system (fig. 21) was tapped first. This part of the magmatic system is represented by the highly evolved pumice fragments obtained from the intracaldera tuffs (fig. 19b). As the eruption progressed deeper levels of the closed system were tapped. Deeper levels are represented by the less evolved pumice fragments obtained from the vent intrusion

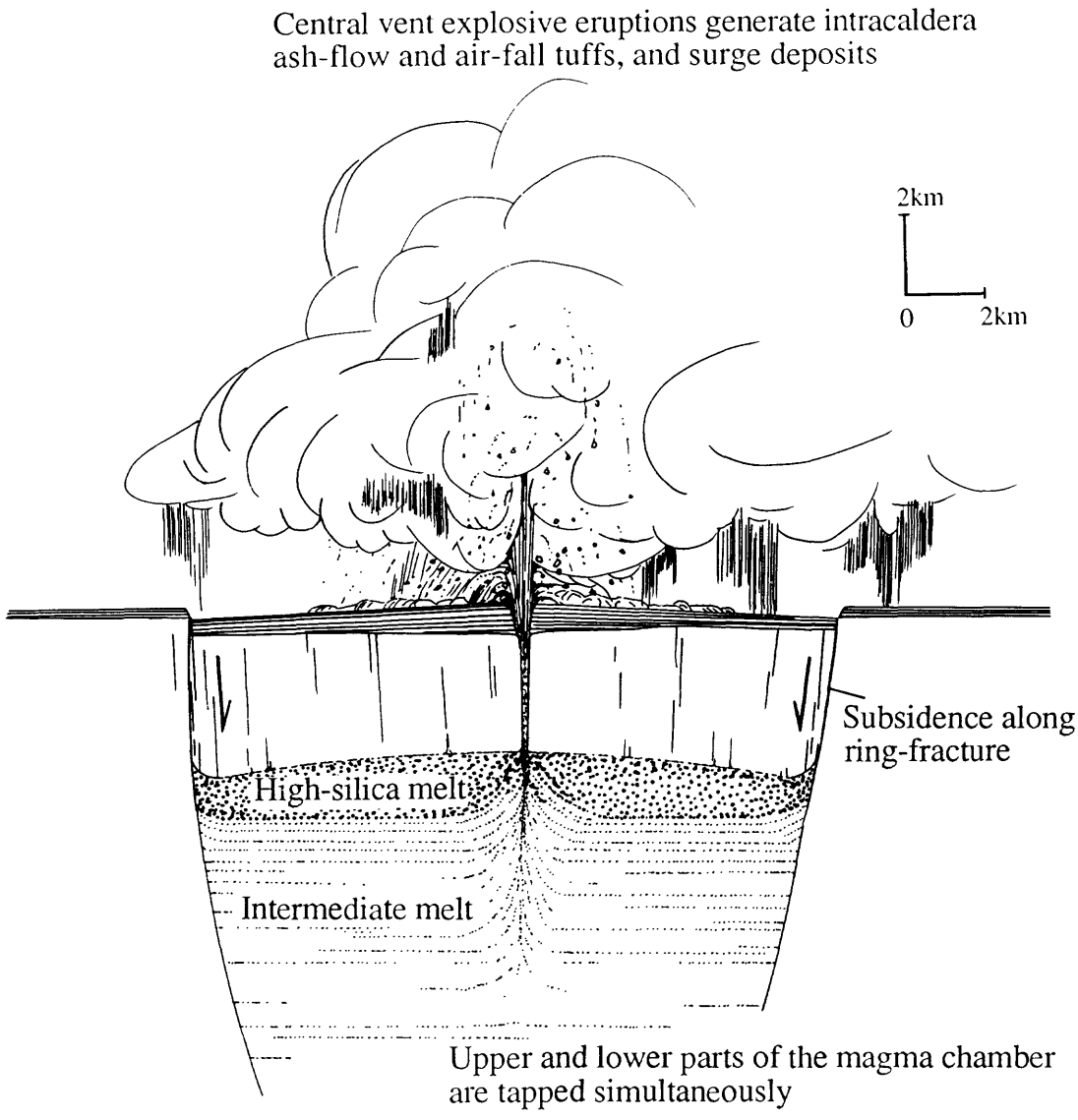

Figure 21. Cartoon sketch illustrating the initial development of the Mahogany Mountain caldera. Explosive eruptions associated with the central vent are shown depositing pyroclastic units within and adjacent to the caldera. As the magma chamber is evacuated the caldera block subsides along the ring-fractures. The high-silica cap and the upper part of the underlying intermediate melt are tapped simultaneously. As the eruption progressed (not shown) deeper levels of less evolved intermediate melt were tapped.

(fig. 19d). Magmatic inclusions are common in all of the exposed caldera-forming units indicating the high-silica cap contributed material throughout the recorded span of the eruption.

SUMMARY

The Mahogany Mountain caldera, Three Fingers caldera, and the Honeycombs volcanic center comprise the Owyhee volcanic field of eastern Oregon. The volcanic field is centered over a north-trending 15- by 35-km, 25 mGal gravity low. The low reflects a subsided mass of caldera-related tuffs and sedimentary rocks.

Three stages of volcanic activity are responsible for the development of the Mahogany Mountain caldera, they are; (1) precaldera lavas, (2) caldera-forming voluminous pyroclastic deposits, and (3) post-caldera resurgent intrusions and lavas. The caldera is one of several volcanic centers in eastern Oregon and north-central Nevada that erupted silicic peralkaline tuff sheets during the middle Miocene. Caldera genesis in this region appears to have coincided with, or immediately preceded the onset of basin-and-range tectonism.

A major central-vent eruption of ash flows and air falls was concurrent with the collapse of the caldera. The vent conduit was subsequently filled with intrusive breccia and rhyolite dikes. The vent complex is presently exposed in the resurgent dome of the caldera.

Geochemical analyses indicate the intracaldera tuffs and vent intrusion tapped a bimodal magmatic system. The system was comprised of a high-silica melt and a zoned intermediate melt. The high-silica cap was an open system that had a small detectable compositional gradient. The underlying intermediate melt was a closed system that developed a steep compositional gradient. A sharp transition zone or compositional interface divided these melts. Field evidence suggests that both parts of the chamber were tapped simultaneously across the compositional interface.

REFERENCES CITED

Boler, F.M., 1979, Aeromagnetic measurements, magnetic source depths, and the Curie point isotherm in the Vale-Owyhee, Oregon, geothermal area: Corvallis, Oregon, Oregon State University, M.S. thesis, 104 p.

Chaplet, Michel, Chorowicz, J., and Roure, F., 1986, Fault patterns by space remote sensing and the rotation of western Oregon during Cenozoic times: Earth and Planetary Science Letters, v. 81, p. 425-433.

Druitt, T.H., and Sparks, R.S.J., 1982, A proximal ignimbrite breccia facies on Santorini, Greece: Journal of Volcanology and Geothermal Research, v. 13, p. 147-171.

Ekren, E.B., Mcintyre, D.H., and Bennet, E.H., 1984, High-temperature, large-volume, lavalike ash-flow tuffs without calderas in southwestern Idaho: U.S. Geological Survey Professional Paper 1272, 76 p.

Fisher, R.V., and Schmincke H.U., 1984, *Pyroclastic Rocks*: Springer-Verlag, 472 p.

Freundt, Armin, Schmincke, H.U., 1985, Lithic-enriched segregation bodies in pyroclastic flow deposits of Laacher See volcano, East Eifel, Germany: Journal of Volcanology and Geothermal Research, v. 25, p. 193-224.

Geometrics Inc., 1979, Aerial gamma ray and magnetic survey - Idaho project, Hailey, Idaho Falls, Elk City quadrangles of Idaho/Montana and Boise quadrangle, Oregon/Idaho, (contract DE-AC13-76GJ01664, subcontract no. 79-323-5): U.S. Department of Energy Open-File Report GJBX-10 (80), [Available through U.S. Geological Survey Branch of Open File Services, Denver, CO], 114 p.

Gray, J.J., Peterson, J.C., Clayton, J., and Baxter, G., 1983, Geology and mineral resources of 18 BLM Wilderness Study Areas, Harney and Malheur Counties, Oregon: Oregon Department of Geology and Mineral Industries, Open-File Report O-83-2, 106 p.

Hildreth, Wes, 1981, Gradients in silicic magma chambers; implications for lithospheric magmatism: Journal of Geophysical Research, v. 86, no. B11, p. 10,153-10,192.

Kittleman, L.R., 1973, Guide to the Geology of the Owyhee Region of Oregon: University of Oregon Museum of Natural History Bulletin 21, 61 p.

Kittleman, L.R., Green, A.R., Hagood, A.R., Johnson, A.M., McMurray, J.M., Russel, R.A., and Weeden, D.A., 1965, Cenozoic stratigraphy of the Owyhee Region, southeastern Oregon: University of Oregon Museum of Natural History Bulletin 1, 45 p.

Kittleman, L.R., Green, A.R., Hagood, A.R., Johnson, A.M., McMurray, J.M., Russel, R.A., and Weeden, D.A., 1967, Geologic map of the Owyhee Region, Malheur County, Oregon: University of Oregon Museum of Natural History Bulletin 8, scale 1:250,000.

Lawrence, R.D., 1976, Strike-slip faulting terminates the Basin and Range province in Oregon: Geological Society of America Bulletin, v. 87, p. 846-850.

Leat, P.T., Macdonald, Ray, and Smith, R.L., 1984, Geochemical evolution of the Menengai volcano, Kenya: Journal of Geophysical Research, v. 89, B10, p. 8571-8592.

Lillie, R.J., 1977, Subsurface geologic structure of the Vale, Oregon, Known Geothermal Resource Area from interpretation of seismic reflection and potential field data: Corvallis, Oregon, Oregon State University, M.S. thesis, 52 p.

Lillie, R.J., and Couch, R.W., 1979, Geophysical evidence of fault termination of the Basin and Range province in the vicinity of the Vale, Oregon, geothermal Area: Basin and Range Symposium and Great Basin Field Conference, p. 175-184.

Lipman, P.W., 1984, The roots of ash-flow calderas in North America; Windows into the tops of granitic batholiths: Journal of Geophysical Research, v. 89, no. B10, p. 8801-8841.

Macdonald, Ray, 1974, Nomenclature and petrochemistry of the peralkaline oversaturated extrusive rocks: Bulletin of Volcanology, v. 38, p. 498-516.

Macdonald, Ray, and Bailey, D.K., 1973, The chemistry of the peralkaline oversaturated obsidians: U.S. Geological Survey Professional Paper 440, p. 1-37.

Mahood, G.A., 1981, A summary of the geology and petrology of the Sierra La Primavera, Jalisco, Mexico: Journal of Geophysical Research, v. 86, no. B11, p. 10,137-10,152.

Mahood, G.A., and Hildreth, Wes, 1983, Large partition coefficients for trace elements in high-silica rhyolites: Geochimica Cosmochimca Acta, v. 47, p. 11-30.

Mahood, G.A., and Hildreth, Wes, 1986, Geology of the peralkaline volcano at Pantelleria, Strait of Sicily: Bulletin of Volcanology, v. 48, p. 143-172.

National Geophysical Data Center, 1984, DMA gravity file of the United States: National Oceanic and Atmospheric Administration, Boulder, Colo., 2 magnetic tapes.

Noble, D.C., 1970, Loss of sodium from crystallized comendite welded tuffs of Miocene Grouse Canyon Member of the Belted Range Tuff, Nevada: Geological Society of America Bulletin, v. 81, p. 2677-2688.

Noble, D.C., McKee, E.H., and Walker G.W., 1974, Pantellerite from the Hart Mountain area, southeastern Oregon; interpretation of radiometric, chemical, and isotope data: U.S. Geological Survey Journal of Research, v. 2, no. 1, p. 25-29.

Plouff, Donald, 1987, Gravity observations by the U.S. Geological Survey in Northwest Nevada, southeast Oregon, and northeast California, 1984-1986: U.S. Geological Survey Open-File Report 87-639, 33 p.

Plumley, P.S., 1986, Volcanic stratigraphy and geochemistry of the Hole in the Ground area, Owyhee Plateau, southeastern Oregon: Moscow, Idaho, University of Idaho, M.S. thesis, 161 p.

Rytuba, J.J., 1981, Relation of calderas to ore deposits in the western United States, *in* Dickinson, W.R., and Payne, W.D., eds., Relation of tectonics to ore deposits in the southern Cordillera: Arizona Geological Society Digest, v. 14, p. 227-236.

Rytuba, J.J., 1989, Volcanism, extensional tectonics, and epithermal mineralization in the northern Basin and Range province, California, Nevada, Oregon, and Idaho, *in* Schindler, K.S., ed., USGS research on mineral resources - program and abstracts: Fifth Annual V.E. McKelvey Forum on Mineral and Energy Resources, U.S. Geological Survey Circular 1035, p. 59-61.

Rytuba, J.J., and McKee, E.H., 1984, Peralkaline ash-flow tuff and calderas of the McDermitt volcanic field, southeast Oregon and north-central Nevada: Journal of Geophysical Research, v. 89, no. B10, p. 8616-8628.

Rytuba, J.J., Vander Meulen, D.B., Plouff, Donald, and Minor, S.A., 1985, Geology of the Mahogany Mountain caldera, Oregon [abs.]: Geological Society of America Abstracts with Programs, v. 17, no. 4, p. 70.

Rytuba, J.J., Vander Meulen, D.B., Minor, S.A., and Harwood, C.S., 1989, Geologic map of the Three Fingers Rock 7.5' quadrangle, Malheur County, Oregon: U.S. Geological Survey Miscellaneous Field Studies Map [in press], scale 1:24,000.

Smith, R.L., 1960, Ash flows: Geological Society of America Bulletin, v. 71, p. 795-842.

Smith, R.L., 1979, Ash flow magmatism, *in* Chapin, C.E., and Elston, W.E., eds., Ash-flow tuffs: Geological Society of America Special Paper 180, p. 5-25.

Smith, R.L., and Bailey, R.A., 1968, Resurgent cauldrons, *in* Studies in volcanology: Geological Society of America Memoir 116, p. 613-662.

Sparks, R.S.J., and Wilson, L., 1976, A model for the formation of ignimbrite by gravitational column collapse: Journal of Geological Society of London, v. 132, p. 441-451.

Swanson, S.E., and Walker, B.M., 1988, Role of the vaper phase in the textural development of porphyry granites; A case study from the Seriate stock, Henderson porphyry molybdenum deposit, Colorado [abs.]: Geological Society of America Abstracts with Programs, v. 3, no. 5672, p. A248.

Vander Meulen, D.B., Rytuba, J.J. Grubensky, M.J., and Goeldener, C.A., 1987a, Geologic map of the Bannock Ridge 7.5' quadrangle, Malheur County, Oregon: U.S. Geological Survey Miscellaneous Field Studies Map MF-1903A, scale 1:24,000.

Vander Meulen, D.B., Rytuba, J.J. Grubensky, M.J., Vercoutere, T.L., and Minor, S.A., 1987b, Geologic map of Pelican Point 7.5' quadrangle, Malheur County, Oregon: U.S. Geological Survey Miscellaneous Field Studies Map MF-1904B, scale 1:24,000.

Vander Meulen, D.B., Rytuba, J.J., King, H.D., and Plouff, Donald, 1987c, Mineral resources of the Honeycombs Wilderness Study Area, Malheur County, Oregon: U.S. Geological Survey Bulletin 1741-A.

Vander Meulen, D.B., Rytuba, J.J. Vercoutere, T.L., and Minor, S.A., 1987d, Geologic map of the Rooster Comb 7.5' quadrangle, Malheur County, Oregon: U.S. Geological Survey Miscellaneous Field Studies Map MF-1902D, scale 1:24,000.

Vander Meulen, D.B., Griscom, Andrew, King, H.D., and Benham, J.R., 1989, Mineral resources of the Upper Leslie Gulch and Slocum Creek Wilderness Study Areas, Malheur County, Oregon: U.S. Geological Survey Bulletin 1741-D.

Vercoutere, T.L., Vander Meulen, D.B., and Minor, S.A., 1987, Geologic map of the Diamond Butte 7.5' quadrangle, Malheur County, Oregon: U.S. Geological Survey Miscellaneous Field Studies Map MF-1901, scale 1;24,000.

Walker, G.W., 1969, Geology of the High Lava Plains province, *in* Mineral and water resources of Oregon: Oregon Department of Geology and Mineral Industries Bulletin 64, p. 77-79.

Walker, G.W., 1970, Cenozoic ash-flow tuffs of Oregon: State of Oregon Department of Geology and Mineral Industries, v. 32, no. 6, p. 97-115.

Walker, G.W., 1977, Geologic map of Oregon east of the 121st meridian: U.S. Geological Survey Miscellaneous Investigations Series Map I-902, scale 1:500,000.

Watson, E.B., 1979, Zircon saturation in felsic liquids: Experimental results and applications to trace element geochemistry: Contributions to Mineralogy and Petrology, v. 70, p. 407-419.

Wohletz, K.H., and Sheridan, M.F., 1979, A model of pyroclastic surge, *in* Chapin, C.E., and Elston, W.E., eds., Ash-flow tuffs: Geological Society of America Special Paper 180, p. 177-194.

Wolff, J.A., 1986, Welded dykes, conduit closure, and lava dome growth at the end of explosive eruptions: Journal of Volcanology and Geothermal Research, v. 28, p. 379-384.